83, 129–135.
138) Meng, L., Mohan, R., Kwok, B. H., Elofsson, M., Sin, N. and Crews, C. M. (1999) Epoxomicin, a potent and selective proteasome inhibitor, exhibits in vivo antiinflammatory activity. Proc. Natl. Acad. Sci. USA **96**, 10403–10408.
139) Adams, J. (2004) The proteasome: a suitable antineoplastic target. Nat. Rev. Cancer **4**, 349–360.
140) Voorhees, P. M. and Orlowski, R. Z. (2006) The proteasome and proteasome inhibitors in cancer therapy. Annu. Rev. Pharmacol. Toxicol. **46**, 189–213.
141) Prudhomme, J., McDaniel, E., Ponts, N., Bertani, S., Fenical, W., Jensen, P. and Le Rock, K. (2008) Marine actinomycetes: a new source of compounds against the human malaria parasite. PloS One **3**, e2335.
142) Yang, H., Landis-Piwowar, K. R., Chen, D., Milacic, V. and Dou, Q. P. (2008) Natural compounds with proteasome inhibitory activity for cancer prevention and treatment. Curr. Protein Pept. Sci. **9**, 227–239.

(Received Sept. 19, 2008; accepted Nov. 28, 2008)

Profile

Keiji Tanaka was born in 1949 and started his research career in 1972 with studies on the amino acid and protein metabolism in the Institute of Enzyme Research, after graduating from the Faculty of Medicine (School of Nutrition) at The University of Tokushima. He received his Ph.D. from The University of Tokushima in 1980, working on the hepatic protein metabolism. He was promoted to assistant professor in 1976 and associate professor in 1995 at the Institute for Enzyme Research at The University of Tokushima, and head of the Department of Molecular Oncology in 1996 and Vice-Director in 2002 at The Tokyo Metropolitan Institute of Medical Science. He is an acting director at The Tokyo Metropolitan Institute of Medical Science since 2006. Over the past 25 years, he focused on elucidating the structure and molecular/physiological functions of the proteasome. The discoveries of proteasomes in 1988, immunoproteasomes in 1994, hybrid proteasomes in 2000, and thymoproteasomes in 2007 are the highlights of his study. His current research interests include intracellular proteolysis mediated by the proteasome, ubiquitin, and autophagy system in eukaryotes in general. He was awarded the Naito Memorial Foundation Prize in 2003, the Asahi Culture Prize and the Uehara Prize in 2004, and the Toray Science Technology Prize in 2007. At present he is a gust professor of Ochanomizu Woman's University, Tokyo Medical and Dental University, The University of Tokyo Graduate School of Frontier Sciences, Juntendo University School of Medicine, and Niigata University School of Medicine.

nature
structural &
molecular biology

Crystal structure of a chaperone complex that contributes to the assembly of yeast 20S proteasomes

Hideki Yashiroda[1,10], Tsunehiro Mizushima[2,10], Kenta Okamoto[3], Tomie Kameyama[1], Hidemi Hayashi[4,5], Toshihiko Kishimoto[5,6], Shin-ichiro Niwa[4], Masanori Kasahara[7], Eiji Kurimoto[3], Eri Sakata[1,3], Kenji Takagi[2], Atsuo Suzuki[2], Yuko Hirano[1], Shigeo Murata[1,8], Koichi Kato[3,9], Takashi Yamane[2] & Keiji Tanaka[1]

Eukaryotic 20S proteasomes are composed of two α-rings and two β-rings, which form an αββα stacked structure. Here we describe a proteasome-specific chaperone complex, designated Dmp1–Dmp2, in budding yeast. Dmp1–Dmp2 directly bound to the α5 subunit to facilitate α-ring formation. In Δ*dmp1* cells, α-rings lacking α4 and decreased formation of 20S proteasomes were observed. Dmp1–Dmp2 interacted with proteasome precursors early during proteasome assembly and dissociated from the precursors before the formation of half-proteasomes. Notably, the crystallographic structures of Dmp1 and Dmp2 closely resemble that of PAC3—a mammalian proteasome-assembling chaperone; nonetheless, neither Dmp1 nor Dmp2 showed obvious sequence similarity to PAC3. The structure of the Dmp1–Dmp2–α5 complex reveals how this chaperone functions in proteasome assembly and why it dissociates from proteasome precursors before the β-rings are assembled.

The 26S proteasome is a large protein complex consisting of a catalytic core particle (the 20S proteasome) and the 19S regulatory particle[1,2]. The 20S proteasome is a cylindrical particle formed by the axial stacking of four heteroheptameric rings: two outer α-rings and two inner β-rings, each of which is made up of seven structurally similar α and β subunits, respectively, interact to create a $\alpha_{1-7}\beta_{1-7}\beta_{1-7}\alpha_{1-7}$ structure.

The molecular mechanisms underlying the assembly of 20S proteasomes have attracted a great deal of interest in recent years. The proteasome from the archaebacterium *Thermoplasma acidophilum* has a quaternary structure that is essentially identical to that of eukaryotic proteasomes, although it is composed of only two different subunits, α and β. Coexpression of these subunits in *Escherichia coli* results in complete and proteolytically active proteasomes[3]. Although deletion of the propeptide of the β subunit has no effect on proteasome assembly in *T. acidophilum*, the assembly of the 20S proteasome in eukaryotes is more complicated; five of the seven β subunits (β1, β2, β5, β6 and β7) are synthesized as precursor forms with extended polypeptide sequences at their N termini, and the propeptides of the β subunits are required for eukaryotic 20S proteasomes to assemble normally[4].

Recent evidence indicates that proteasome assembly in eukaryotes requires additional chaperone molecules. In mammals, a heterodimer of proteasome-assembling chaperones 1 and 2 (PAC1-PAC2) binds to early assembly intermediates containing a restricted subset of α subunits and promotes α-ring formation[5]. PAC1-PAC2 remains attached to the α-ring after its formation and suppresses nonproductive α-ring dimerization, thereby promoting attachment of the β subunits to the α-rings. β subunits are thought to attach to the α-rings in an orderly manner in mammals as well as in yeast; in fact, incomplete precursor complexes consisting of all seven α subunits and three β subunits (β2, β3 and β4) have been identified[6,7]. Another chaperone molecule, known as the proteasome maturation factor Ump1, associates with 15S proteasome precursors[8]. In the yeast Δ*ump1* mutant, proteasome assembly and maturation are strongly impaired. In a similar way to PAC1-PAC2, a newly identified mammalian chaperone, PAC3, was also found to bind to the α-ring and to be required for proper α-ring formation[9]. Unlike PAC1-PAC2 and Ump1, however, PAC3 dissociates before the formation of half-proteasomes, a process that is coupled with the recruitment of the β subunits and Ump1.

Whether eukaryotic cells share a common mechanism for proteasome assembly is unknown. Yeast cells express Ump1 with about 30% amino acid sequence identity with the human counterpart (also called POMP and proteassemblin)[10–12], suggesting that Ump1 is probably conserved in eukaryotes. As for the PAC proteins, it was recently

[1]Laboratory of Frontier Science, Core Technology and Research Center, Tokyo Metropolitan Institute of Medical Science, Bunkyo-ku, Tokyo 113-8613, Japan. [2]Department of Biotechnology, Graduate School of Engineering, Nagoya University, Chikusa-ku, Nagoya 464-8603, Japan. [3]Department of Structural Biology and Biomolecular Engineering, Graduate School of Pharmaceutical Sciences, Nagoya City University, 3-1 Tanabe-dori, Mizuho-ku, Nagoya 467-8603, Japan. [4]Link Genomics, Inc., Chuo-ku, Tokyo 103-0024, Japan. [5]Proteome Analysis Center and [6]Department of Biomolecular Science, Faculty of Science, Toho University, Funabashi, Chiba 274-8510, Japan. [7]Department of Pathology, Hokkaido University Graduate School of Medicine, Sapporo, Hokkaido 060-8638, Japan. [8]Laboratory of Protein Metabolism, Graduate School of Pharmaceutical Sciences, the University of Tokyo, 7-3-1 Hongo, Bunkyo-ku, Tokyo 113-0033, Japan. [9]Institute for Molecular Science, National Institutes of Natural Sciences, 5-1 Higashi-yama, Myodaiji, Okazaki 444-8787, Japan. [10]These authors contributed equally to this work. Correspondence should be addressed to K. Tanaka (tanakak@rinshoken.or.jp).

Received 20 August 2007; accepted 9 January 2008; published online 17 February 2008; doi:10.1038/nsmb.1386

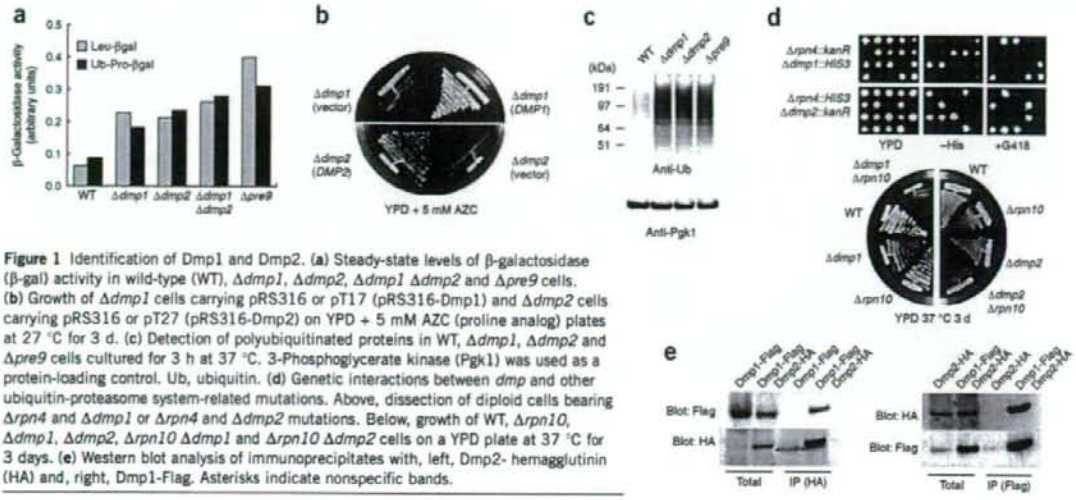

Figure 1 Identification of Dmp1 and Dmp2. (**a**) Steady-state levels of β-galactosidase (β-gal) activity in wild-type (WT), Δ*dmp1*, Δ*dmp2*, Δ*dmp1* Δ*dmp2* and Δ*pre9* cells. (**b**) Growth of Δ*dmp1* cells carrying pRS316 or pT17 (pRS316-Dmp1) and Δ*dmp2* cells carrying pRS316 or pT27 (pRS316-Dmp2) on YPD + 5 mM AZC (proline analog) plates at 27 °C for 3 d. (**c**) Detection of polyubiquitinated proteins in WT, Δ*dmp1*, Δ*dmp2* and Δ*pre9* cells cultured for 3 h at 37 °C. 3-Phosphoglycerate kinase (Pgk1) was used as a protein-loading control. Ub, ubiquitin. (**d**) Genetic interactions between *dmp* and other ubiquitin-proteasome system-related mutations. Above, dissection of diploid cells bearing Δ*rpn4* and Δ*dmp1* or Δ*rpn4* and Δ*dmp2* mutations. Below, growth of WT, Δ*rpn10*, Δ*dmp1*, Δ*dmp2*, Δ*rpn10* Δ*dmp1* and Δ*rpn10* Δ*dmp2* cells on a YPD plate at 37 °C for 3 days. (**e**) Western blot analysis of immunoprecipitates with, left, Dmp2- hemagglutinin (HA) and, right, Dmp1-Flag. Asterisks indicate nonspecific bands.

reported that in *Saccharomyces cerevisiae* Pba1 and Pba2, which show weak sequence similarity to PAC1 and PAC2, respectively, form a heterodimeric complex and bind to proteasome precursor complexes[7]. Unlike the phenotypes observed following PAC1 and PAC2 knockdowns, however, Δ*pba1* and Δ*pba2* cells show only mild defects in proteasome biogenesis.

In this paper, we describe a newly identified heterodimeric complex of Dmp1–Dmp2. Although Dmp1 and Dmp2 show no obvious sequence similarities to PAC3, the biological function and quaternary structure of this heterodimer are strikingly similar to those of PAC3. We show that Dmp1–Dmp2 is critically involved in 20S proteasome assembly, and we propose that the identified chaperone-dependent mechanisms that contribute to proteasome assembly are probably conserved among eukaryotes.

RESULTS

Isolation of *dmp* mutants

To search for genes involved in the ubiquitin-proteasome system, we streaked yeast knockout strains on YPD plates containing the proline analog L-azetidine-2-carboxylic acid (AZC; 5 mM) or SD plates containing the arginine analog canavanine (1 mg ml^{-1}) and incubated them at 26 °C for 3 d. Among the many mutants that were sensitive to the amino acid analogs, we selected 23 uncharacterized mutants on the basis of the criterion that the disrupted gene products or proteins that they interact with are conserved in higher eukaryotes. We then examined the ability of each mutant to degrade model substrates for the N-end rule pathway or the ubiquitin fusion degradation (UFD) pathway[13,14]. Because Δypl144w cells showed the most severe defect among the 23 selected mutants, we further examined the Δypl144w strain, which we named Δ*dmp1* (for degradation of misfolded proteins 1; **Fig. 1a, Supplementary Methods** and **Supplementary Fig. 1** online). We confirmed degradation defects in Δ*dmp1* cells by cycloheximide-chase experiments of Gcn4, a transcription activator that turns over rapidly in rich medium[15] (**Supplementary Fig. 1**). We cloned the YPL144W gene, including the 5′ and 3′ flanking regions, into the pRS316 single-copy vector. Because cloned YPL144W complemented the growth defect of the Δ*dmp1* cells on YPD + 5 mM AZC plates, we concluded that YPL144W was *DMP1* (**Fig. 1b**), which encodes a 148-residue (16.6 kDa) protein. We also confirmed that deletion of *DMP1* resulted in the stabilization of model substrates in another background strain, W303 (**Supplementary Fig. 1**).

Next we examined the accumulation of polyubiquitinated proteins in the Δ*dmp1* mutant. We used Δ*pre9* cells, which lacked the α3 subunit of the 20S proteasome, as a positive control. A larger amount of polyubiquitinated proteins accumulated in Δ*dmp1* cells than in wild-type cells, whereas the levels in Δ*dmp1* and Δ*pre9* cells were comparable (**Fig. 1c**). This result indicated that the ubiquitin-dependent degradation mediated by the 26S proteasome was impaired in Δ*dmp1* cells.

To further confirm that Dmp1 is involved in the ubiquitin-proteasome pathway, we crossed the Δ*dmp1* strain with strains carrying mutations affecting the ubiquitin-proteasome system. Rpn4 (also known as Son1 or Ufd5) is a transcriptional activator of genes encoding proteasome subunits[16,17], whereas Rpn10 (the mammalian S5a homolog) acts as a receptor capable of trapping polyubiquitinated proteins[18]. When we crossed Δ*dmp1* with Δ*rpn4*, no double mutants were obtained from 6 predicted tetratypes and 2 nonparental ditypes in tetrad analysis of 11 asci (**Fig. 1d** and data not shown). In contrast, Δ*dmp1* Δ*rpn10* double mutants were viable, but showed synthetic growth defects at high temperatures (**Fig. 1d**). These genetic interactions suggested that the ubiquitin-proteasome pathway was impaired in Δ*dmp1* cells.

Identification of Dmp1-interacting proteins

To identify proteins that interact with Dmp1, we generated a strain expressing C-terminally Flag-tagged Dmp1 from its native promoter and analyzed anti-Flag immunoprecipitates using MS. We identified three interacting proteins: one previously unknown protein encoded by YLR021W as well as the α5 (Pup2) and α6 (Pre5) subunits of the 20S proteasome (**Supplementary Fig. 2** online). Because the disruptant of the previously unknown protein displayed AZC sensitivity similar to the Δ*dmp1* strain, we named the YLR021W gene product Dmp2 (**Fig. 1b**). Dmp2 consists of 179 amino acid residues and has a molecular mass of 20.1 kDa. In addition to AZC sensitivity,

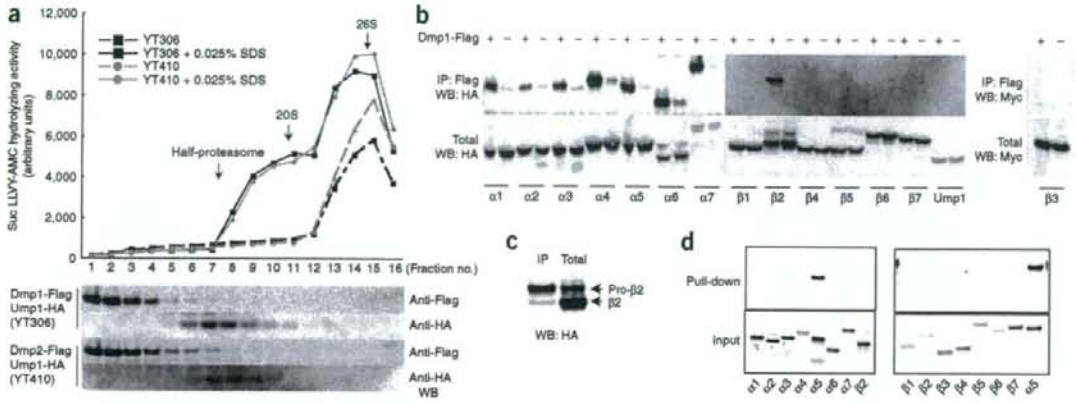

Figure 2 Characterization of the Dmp1–Dmp2 complex. (**a**) Suc-LLVY-AMC hydrolyzing activity of cell lysates fractionated by glycerol gradient centrifugation (above) and immunoblotted (WB) with anti-Flag or anti-hemagglutinin (HA) antibodies (below). The three arrows depict the locations of half-proteasomes, 20S proteasomes and 26S proteasomes. (**b**) Detection of coimmunoprecipitated (IP) proteasome subunits with Dmp1-Flag. (**c**) Comparison of the β2 subunit in the total lysate or immunoprecipitate with Dmp1-Flag. (**d**) Binding assay of recombinant GST-Dmp1–Dmp2 and the 20S proteasome subunits translated and ^{35}S-radiolabeled in reticulocyte lysates.

Δ*dmp2* cells showed the same phenotypes as Δ*dmp1* cells, including the stabilization of model substrates and accumulation of polyubiquitinated proteins (**Fig. 1a,c**). Furthermore, we observed synthetic lethality and high temperature sensitivity when Δ*dmp2* cells were crossed with Δ*rpn4* and Δ*rpn10* cells, respectively (**Fig. 1d**).

Next, to examine the interaction between Dmp1 and Dmp2 *in vivo*, Dmp2 was C-terminally tagged with hemagglutinin (HA). Dmp2-3×HA was immunoprecipitated from cell extracts using anti-HA antibodies. Western blots of the immunoprecipitated material using anti-Flag antibodies revealed that Dmp1-3×Flag was also present (**Fig. 1e**). Conversely, when Dmp1-3×Flag was immunoprecipitated using anti-Flag antibodies, Dmp2-3×HA was coimmunoprecipitated (**Fig. 1e**). To further confirm that Dmp1 and Dmp2 form a complex, 6×His-Dmp1 and Dmp2 were coexpressed in *E. coli* and purified using nickel-agarose beads. Dmp1 and Dmp2 formed a complex with an apparent 1:1 stoichiometry and a relative molecular mass of 43 kDa, indicating that the complex was a heterodimer (**Supplementary Fig. 3** online).

We then examined whether the Δ*dmp1* phenotype was enhanced by the deletion of *DMP2*. The Δ*dmp1* Δ*dmp2* double mutant was viable, and, compared to the single mutants, the double deletion did not enhance the stabilization of model substrates (**Fig. 1a**). This result implies that Dmp1 and Dmp2 function as a complex, and that the deletion of either protein was sufficient to eliminate the function of the heterodimeric complex.

Dmp1–Dmp2 binds to 20S proteasome precursors

To further characterize the interaction between Dmp1–Dmp2 and the proteasome subunits, cell extracts of strains expressing Ump1-HA and Dmp1-3×Flag or Dmp2-3×Flag were fractionated using 8–32% (v/v) glycerol density-gradient centrifugation. The Dmp1–Dmp2 complex and half-proteasomes containing Ump1 were detected on western blots using anti-Flag and anti-HA antibodies (**Fig. 2a**, below). Peptidase activity in each fraction was also measured to determine the distributions of the 20S and 26S proteasomes (**Fig. 2a**, above). A low concentration of SDS (0.025% (w/v)) is known to act as an artificial activator of 20S proteasomes that are usually latent in cells. This allowed us to discriminate the activity of 20S proteasomes from that of 26S proteasomes. Both Dmp1-3×Flag and Dmp2-3×Flag were primarily observed in fractions 1–4, whereas Ump1-HA was found in fractions 7–10, and 20S and 26S proteasomes were identified in fractions 10–12 and 14–15, respectively. This result indicates that the Dmp1–Dmp2 complex does not bind to the α subunits either in the half-proteasomes or in mature proteasomes.

To examine whether the Dmp1–Dmp2 complex bound specifically to α5 and α6 *in vivo*, all of the α and β subunits except β3 and Ump1 were C-terminally tagged with HA. Adding a 3×HA tag onto the C terminus of β3 caused lethality, so we constructed a strain expressing N-terminally Myc-tagged β3 under the control of the *GAL1* promoter. As shown in **Figure 2b**, when Dmp1-3×Flag was immunoprecipitated using anti-Flag M2 agarose beads, all of the α subunits were pulled down with Dmp1-3×Flag. In contrast, of the β subunits, only β2 was pulled down. Intriguingly, β2 coimmunoprecipitated as its precursor form, which was verified by comparing the coimmunoprecipitated form with β2 in the total cell lysate (**Fig. 2c**). No interaction between Ump1 and Dmp1 was detected (**Fig. 2b**). These results indicate that assembly of the 20S proteasome proceeds via a precursor complex composed of the α-ring, β2 and Dmp1–Dmp2, and that the Dmp1–Dmp2 complex dissociates from precursors before the formation of half-proteasomes containing Ump1.

We then investigated which of the proteasome subunits bind directly to Dmp1–Dmp2. Glutathione S-transferase (GST)–tagged Dmp1–Dmp2 (GST–Dmp1–Dmp2) bound to only the α5 subunit among the α and β subunits, and Ump1 translated *in vitro* (**Fig. 2d**). This result indicated that the Dmp1–Dmp2 complex bound to the proteasome precursors via direct interactions with the α5 subunit.

Impairment of 20S proteasome assembly in Δ*dmp1* cells

We then examined the Δ*dmp1* phenotype in more detail, focusing on proteasome biogenesis. Extracts from wild-type or Δ*dmp1* cells were fractionated using 8–32% (v/v) glycerol gradient centrifugation, and the peptidase activity of each fraction was measured with or without 0.025% (w/v) SDS (**Fig. 3a**). This experiment revealed that the 20S proteasome activity was reduced by approximately 60% in Δ*dmp1*

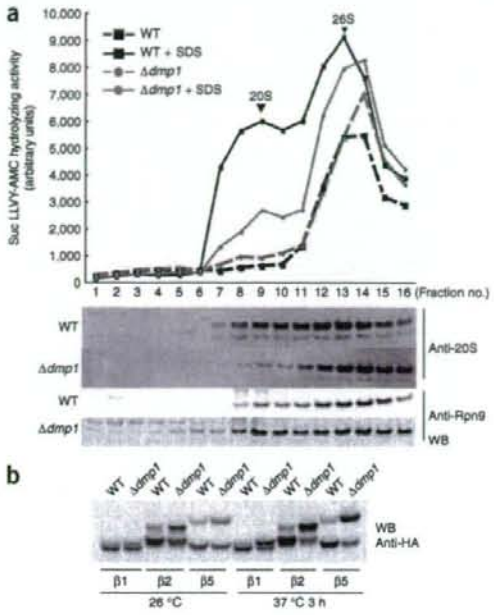

Figure 3 Impaired 20S proteasome assembly in Δ*dmp1* cells. (**a**) Suc-LLVY-AMC hydrolyzing activity of proteasomes in wild-type (WT) and Δ*dmp1* cells and immunoblotted (WB) with anti-20S (above) or anti-Rpn9 (below) antibodies. Arrowheads indicate the positions of 20S or 26S proteasomes. (**b**) WB analysis of HA-tagged β subunits in WT and Δ*dmp1* cells.

cells compared to wild-type cells. Immunoblot analysis using an antibody to yeast 20S confirmed that the level of 20S proteasome was lower in Δ*dmp1* cells (**Fig. 3a**, below). For Δ*dmp1* cells, the bands representing the 20S proteasome were faint in fractions 7–10. Conversely, the bands representing the lid component Rpn9 were slightly stronger in the fractions from Δ*dmp1* cells than in those from wild-type cells (**Fig. 3a**, below). The level of free 19S regulatory particle complexes may have increased in Δ*dmp1* cells as a result of the shortage of 20S proteasomes.

The impairment of 20S proteasome assembly in Δ*dmp1* cells was supported by the observation that the propeptides of the β subunits were not efficiently cleaved in these cells. This phenotype was more apparent at elevated temperatures (**Fig. 3b**).

Dmp1–Dmp2 is involved in α-ring formation

We further examined the involvement of the Dmp1–Dmp2 complex in proteasome biogenesis. Total cell lysates from wild-type, Δ*dmp1*, Δ*dmp2*, Δ*blm10* and Δ*pba2* cells were subjected to blue native PAGE (BN-PAGE) (**Fig. 4a**). Blm10 has been reported to be involved in a late stage of nuclear proteasome assembly and to function as a proteasome activator, although these findings remain controversial[19,20]. Pba2 has weak amino acid–sequence similarity to mammalian PAC2 (refs. 5,7). In agreement with the decreased 20S proteasome activity (**Fig. 3a**), the level of 20S proteasomes was lower in Δ*dmp1* and Δ*dmp2* cells, whereas no appreciable decrease was observed for Δ*pba2* or Δ*blm10* cells. Notably, in addition to the decrease in the level of 20S proteasomes, we observed other quickly migrating bands in the samples from Δ*dmp1* and Δ*dmp2* cells. To identify these bands, we carried out BN-PAGE and western blot analysis using strains expressing HA-tagged proteasome subunits. The results revealed that the quickly migrating bands contained all of the α subunits except α4, together with β2 (**Fig. 4b**). Tagging β6 with HA seemed to affect the assembly of the 20S proteasome, because the resulting band pattern was different from those observed from the strains expressing other tagged subunits (data not shown). Furthermore, it is noteworthy that anti-HA antibodies did not recognize the α7 subunit in mature proteasomes, whereas it clearly stained the subunit in the intermediate band, suggesting that the C-terminal portion of the α7 subunit is cleaved during maturation of the β-ring. To confirm that α4 was not part of the quickly migrating band observed in samples from Δ*dmp1* cells and to eliminate the possibility

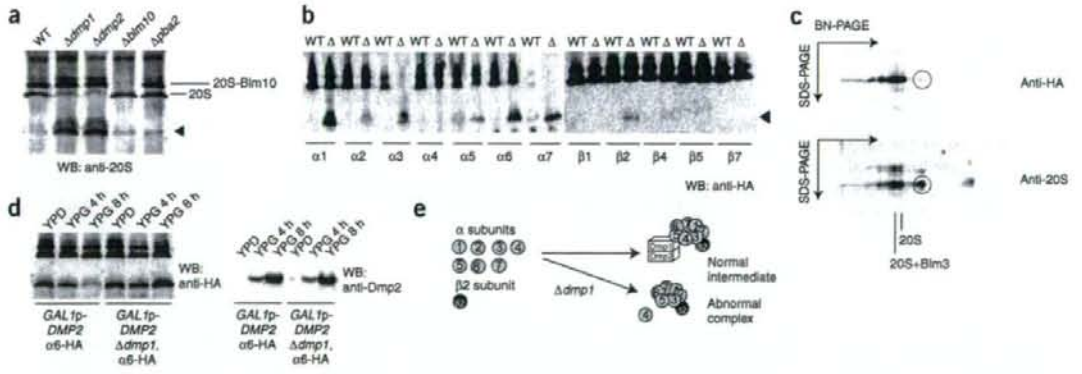

Figure 4 Detection of abnormal α-rings lacking α4 in Δ*dmp1* and Δ*dmp2* cells. Blue native (BN)-PAGE and immunoblotting (WB) with anti-20S proteasome (**a**) or anti- hemagglutinin (HA) antibodies (**b**). The filled arrowhead denotes intermediates composed of α-rings observed in Δ*dmp1* and Δ*dmp2* cells. Δ in **b** denotes Δ*dmp1*. Note in **b** that the C-terminally attached HA tag of α7 may not be present in mature proteasomes in both wild-type (WT) and Δ*dmp1* cells. (**c**) Two-dimensional BN–SDS-PAGE analysis of the proteasome in YT334 (Δ*dmp1*, α4-HA) cells. Circles denote the position of a quickly migrating band observed only in Δ*dmp1* and Δ*dmp2* cells. (**d**) Detection of abnormal complex by BN-PAGE and immunoblotting (left). Detection of Dmp2 by SDS-PAGE and immunoblotting (right). (**e**) Schematic model for Dmp1–Dmp2 function. Dmp1–Dmp2 is required for the efficient construction of the α-ring. The details of the model are provided in the text.

that the HA epitope of α4-HA was buried and inaccessible to the anti-HA antibodies, we conducted two-dimensional BN-PAGE–SDS-PAGE; the results confirmed that α4 was indeed absent from this complex (**Fig. 4c**). We then examined whether this complex was a normal intermediate or an abnormal complex using the strains in which *DMP2* is under the control of the galactose-inducible promoter. When the expression of *DMP2* was repressed in YPD medium, quickly migrating bands were observed as expected (**Fig. 4d**). If this complex is a normal intermediate, which can be detected only when the assembly step is slowed by the lack of Dmp2, it is expected to be diminished promptly when the Dmp2 proteins are supplied again. However, this complex remained even 4 h after the expression of *DMP2* was induced (**Fig. 4d**). This result suggests that the lack of Dmp1–Dmp2 results in nonproductive complexes and that the Dmp1–Dmp2 complex ensures that the steps underlying proteasome assembly occur in the proper order (**Fig. 4e**). Dmp1–Dmp2 is required for the efficient construction of α-rings and in particular for the incorporation of α4 into the α-rings.

Overall structure of the Dmp1–Dmp2 complex

To examine the structural basis of the function of this chaperone, the crystal structure of the Dmp1–Dmp2 complex was determined using multiwavelength anomalous dispersion and refined to 1.96-Å resolution (**Fig. 5a**). Dmp1 has a globular structure consisting of a six-stranded β-sheet and three α-helices. Two antiparallel sheets ($S_1$1, $S_1$2, $S_1$3 and $S_1$4, $S_1$5, $S_1$6) are composed of three β-strands joined by a parallel interaction between one strand from each sheet ($S_1$3 and $S_1$6). $H_1$1 and $H_1$3 are bound on one side of the β-sheet, and one short helix ($H_1$2) is located between $S_1$6 and $H_1$3. Dmp2, which has a globular structure similar to that of Dmp1, consists of a six-stranded β-sheet and four α-helices. Although no obvious amino acid–sequence similarity between Dmp1 and Dmp2 was observed, the tertiary structure of Dmp2 closely resembles that of Dmp1, with an average r.m.s. deviation of 3.0 Å for 103 Cα atoms (**Fig. 5a**). The loop between $S_1$4 and $S_1$5 of Dmp1 (residues 68–77), however, is distinct from the same loop in Dmp2 (residues 60–90 between $S_2$4 and $S_2$5 of Dmp2). The loop in Dmp2 is larger than that in Dmp1 and is part of a protruding structure that also contains $H_2$1 and a flexible region. The $H_2$1 helix is stabilized by a crystal contact.

The Dmp1–Dmp2 heterodimer has a β-sandwich structure formed by two six-stranded β-sheets consisting of strands $S_1$1–$S_1$6 of Dmp1 and $S_2$1–$S_2$6 of Dmp2 (**Fig. 5a,b**). This sandwich structure is surrounded by helices $H_1$1 and $H_1$3 of Dmp1 on one side and $H_2$2 and $H_2$4 of Dmp2 on the other side. Dmp1 and Dmp2 interact through an extensive interface that is approximately 25 Å long and 22 Å wide, burying a total of 2,318 Å^2 of surface area (1,159 Å^2 each for Dmp1 and Dmp2). The interface involves β-strands $S_1$1-$S_1$6, loop $S_1$2-$S_1$3 and loop $S_1$3-$S_1$4 of Dmp1, which interact against β-strands $S_2$1-$S_2$6, loop $S_2$2-$S_2$3 and loop $S_2$3-$S_2$4 of Dmp2. Dmp1–Dmp2 binding is mediated by both hydrogen bonds and van der Waals contacts (**Fig. 5c**). Residues involved in intermolecular formation of hydrogen bonds are Leu2, Pro37, Ser39, Ser53, Ser54, Leu56, Tyr59 and Leu85 of Dmp1 (located in strands $S_1$1, $S_1$3, $S_1$4 and $S_1$5, and loop $S_1$3-$S_1$4) and Glu26, Asn35, Asn36, Gln41, Arg43, Lys100 and Ser144 of Dmp2 (located in strands $S_2$2, $S_2$3, $S_2$5 and $S_2$6, and loop $S_2$2 -$S_2$3). Although the interface residues are not well conserved between Dmp1 and Dmp2, they occupy similar positions in the three-dimensional structure of each Dmp molecule (**Fig. 5d**).

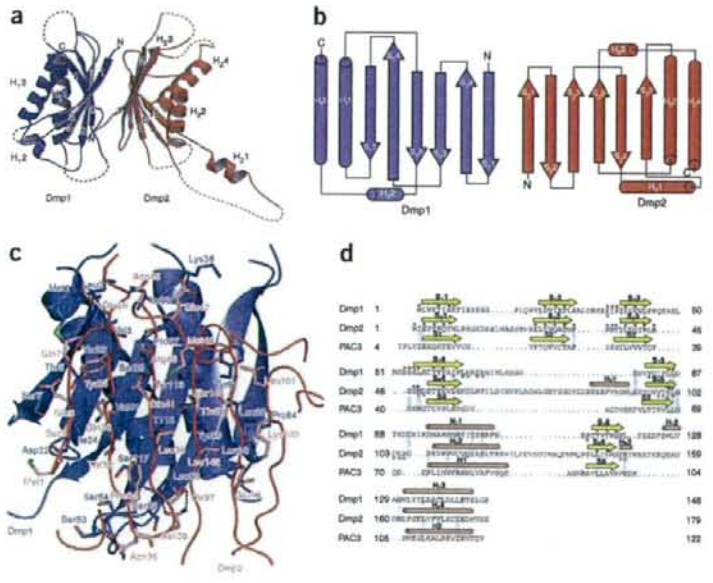

Figure 5 Structure of the Dmp1–Dmp2 complex. (**a**) A ribbon diagram of the Dmp1–Dmp2 complex. Dmp1 and Dmp2 are colored blue and red, respectively. The secondary structural elements are labeled. Dotted lines represent disordered regions. (**b**) Topology diagram of the Dmp1–Dmp2 complex. The α helices and β strands are represented by cylinders and arrows, respectively. (**c**) Close-up view of the Dmp1–Dmp2 interface showing amino acids of Dmp1 (blue) and Dmp2 (red). Hydrogen bonds are indicated by dotted lines. (**d**) Structure-based sequence alignments of Dmp1, Dmp2 and PAC3. The secondary structural elements of Dmp1, Dmp2 and PAC3 are indicated above the alignments. Identical or highly conserved residues are highlighted with a blue background. Residues that interact with Dmp2, Dmp1 and α5 are indicated by red dots, purple dots and green stars, respectively.

Structure of the Dmp1–Dmp2–α5 complex

The Dmp1–Dmp2 complex directly interacted with the α5 subunit (**Fig. 2d**). To understand the binding of Dmp1–Dmp2 to α5, we first constructed a mutant version of Dmp2 (Dmp2 Δloop), in which the protruding region (residues 61–90) was deleted to facilitate crystallization. The crystal structure of the Dmp1–Dmp2 Δloop–α5 complex was determined at 2.9-Å resolution (**Fig. 6a**, above). The structure of α5, which consists of five α-helices and ten β-strands, is essentially identical to the previously reported structure of the α5 subunit in the 20S proteasome complex; these structures have an average r.m.s. deviation of 0.79 Å for the Cα positions. The H0 helix of α5, however, is disordered in the Dmp1–Dmp2 Δloop-α5 complex (**Fig. 6a**, above). The Dmp1–Dmp2 Δloop structure in the Dmp1–Dmp2 Δloop–α5 complex can be superposed on the Dmp1–Dmp2 structure with an average r.m.s. deviation of 0.93 Å for the Cα positions, indicating that α5 binding does not cause substantial structural changes in the Dmp1–Dmp2 complex. The Dmp1–Dmp2 Δloop complex and

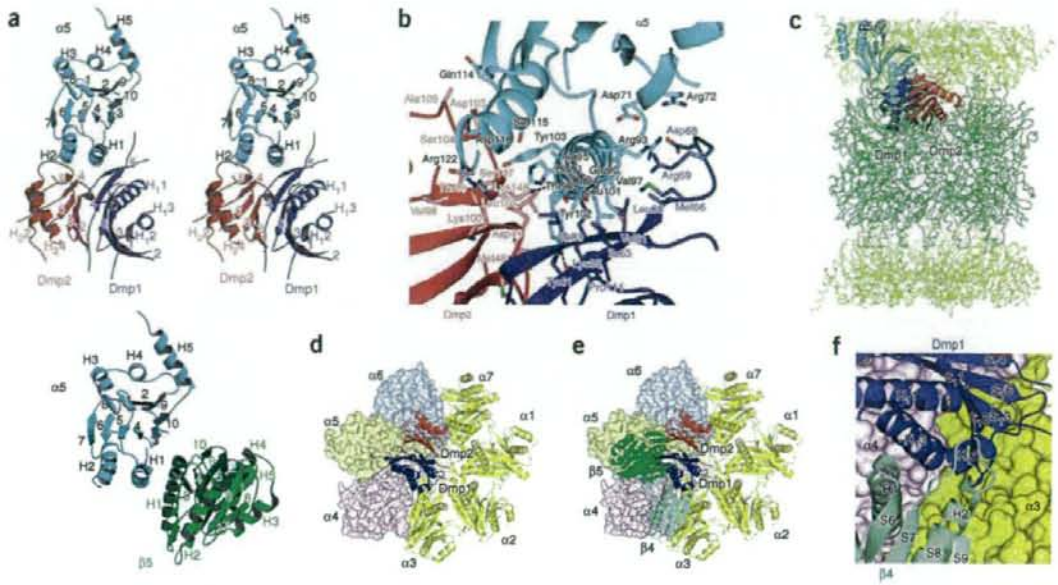

Figure 6 Structure of the Dmp1–Dmp2–α5 complex. (**a**) Above, a stereo ribbon diagram of the Dmp1–Dmp2 Δloop-α5 complex. Dmp1, Dmp2 Δloop and α5 are colored blue, red and cyan, respectively. Below, a ribbon diagram of the α5 (PDB ID code: 1RYP; chain E, cyan) and β5 (PDB ID code: 1RYP; chain L, green) complex. The secondary structural elements are labeled. (**b**) Close-up view of the Dmp1–Dmp2 Δloop–α5 interface showing amino acids of Dmp1 (blue), Dmp2 (red) and α5 (cyan). Hydrogen bonds are indicated by dotted lines. (**c**) Binding positions of the Dmp1–Dmp2 complex in the 20S proteasome. Dmp1, Dmp2 and α5 are shown as ribbon representations and are colored blue, red and cyan, respectively. Cα traces are colored yellow in the α-ring and green in the β-ring. (**d**) Model of the Dmp1–Dmp2–α-ring complex derived from the published structure of the yeast proteasome (PDB ID code: 1RYP). Dmp1, Dmp2 and the α-ring (α1, α2, α3 and α7) are shown as ribbon representations and are colored blue, red and yellow, respectively. α4 (violet), α5 (light yellow) and α6 (light blue) are shown as surface plots. (**e**) Model of the Dmp1–Dmp2–α-ring–β4–β5 complex. β4 and β5 are shown as ribbon representations and are colored light green and green, respectively. (**f**) Close-up view of the interface between Dmp1 and β4 in the model of the complex.

α5 are bound by interactions of $S_1$4, $S_1$5 and loops $S_1$2-$S_1$3, $S_1$4-$S_1$5, and $H_1$1-$S_1$6 of Dmp1; $H_2$3, $S_2$5 and loops $S_2$3-$S_2$4 and $S_2$5-$H_2$2 of Dmp2; and helices H1 and H2 of α5. The truncated loop of Dmp2 is located on the opposite side of α5. A total of 984 Å^2 of accessible surface area (557 Å^2 for Dmp1 and 427 Å^2 for Dmp2) is buried at the interface between the Dmp1–Dmp2 Δloop complex and α5. The α5 subunit binds to Dmp1–Dmp2 by packing its H1 helix against the concave surface of the Dmp1–Dmp2 complex (**Fig. 6a**, above, and **Fig. 6b**). The surface area occupied by the H1 helix of the Dmp1–Dmp2 complex is 692 Å^2. Glu90, Thr94, Val97, Leu101, Tyr102, Tyr103 and Arg122 of α5 have a central role, making multiple van der Waals contacts to Dmp1 and Dmp2. Thr94, Val97 and Tyr102 are not conserved among the α subunits of yeast proteasomes; these residues might be important for specific interactions between α5 and the Dmp1–Dmp2 complex. The intermolecular hydrogen bonds are formed by residues Tyr102, Tyr103, Asp118 and Arg122 of α5, Lys35 of Dmp1 and Met48, Thr99, Ser104, Ser147 and Lys148 of Dmp2.

The structure of the Dmp1–Dmp2 Δloop–α5 complex illustrates an intermediate state of proteasome assembly. A model of Dmp1–Dmp2 interacting with the α-ring was generated by superimposing the α5 subunit from Dmp1–Dmp2 Δloop–α5 on the structure of the 20S proteasome (PDB ID code 1RYP). In this model, Dmp1–Dmp2 bound to the inner surface of the α-ring (**Fig. 6c,d**). The Dmp1–Dmp2 binding sites in the α-ring are located more internally than those that interact with the β subunits (**Fig. 6e**). The β2, β3 and β4 subunits of the proteasomes are thought to attach to the α-rings during the primary stage of β-ring assembly. In the Dmp1–Dmp2–α-ring model, attachment of the β4 subunit to the α-ring causes steric hindrance between β4 and Dmp1 (**Fig. 6e,f**). This steric hindrance probably triggers the release of Dmp1–Dmp2 from the α-ring during the attachment of the β subunits onto the α-ring.

Structural similarity between Dmp1, Dmp2 and PAC3

The functional features of the Dmp1–Dmp2 complex discussed above are reminiscent of mammalian PAC3. PAC3 is involved in α-ring formation and is released from precursor complexes before the formation of half-proteasomes. To examine whether Dmp1–Dmp2 and PAC3 are structurally similar, we determined the crystal structure of PAC3 at 2.0-Å resolution. In the crystal, PAC3 forms a homodimer related by pseudo two-fold symmetry (**Fig. 7a**). Notably, the tertiary structure of PAC3 is strikingly similar to those of Dmp1 and Dmp2 (**Fig. 7b**). PAC3 assumes a fold composed of one six-stranded β-sheet and two α-helices: H1 and H2 (**Fig. 7c**). Superposition of PAC3 on Dmp1 and Dmp2 resulted in an average r.m.s. deviation of 3.2 Å for 107 Cα atoms and 2.0 Å for 111 Cα atoms, although no obvious sequence similarity was found even when the alignment was made on the basis of experimentally verified secondary structures (**Fig. 5d**). Comparison of the structures of Dmp1, Dmp2 and PAC3 with other known protein structures using the DALI server yielded no proteins with marked structural similarities.

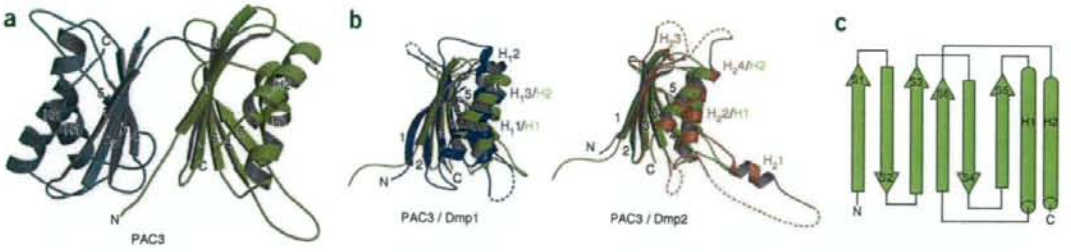

Figure 7 Structural similarity between Dmp1–Dmp2 and the human PAC3. (**a**) Structure of PAC3. A ribbon diagram of the PAC3 homodimer. Molecule A and molecule B are colored dark cyan and olive, respectively. The secondary structural elements of PAC3 are labeled. (**b**) The structure of PAC3 (olive) is compared with the structures of Dmp1 (blue) and Dmp2 (red). The secondary structural elements are labeled. (**c**) Topology diagram of PAC3. α-Helices and β-strands are represented by cylinders and arrows, respectively.

DISCUSSION

We have identified the Dmp1–Dmp2 complex as a proteasome-assembling chaperone in budding yeast. Dmp1–Dmp2 binds to proteasome subunits until they are organized into precursor complexes consisting of an α-ring and a β2 subunit and dissociates by the time the precursors become half-proteasomes, which consist of one copy of each α- and β-ring.

Whereas α-ring formation in mammals is driven by a concerted action of several chaperones (that is, the PAC1-PAC2 heterodimer and PAC3)[5,9], Dmp1 and Dmp2 are the first chaperone molecules shown to be involved in α-ring formation in yeast. Although neither Dmp1 nor Dmp2 is essential for normal growth, self-assembly of 20S proteasomes may be less efficient in the absence of Dmp1–Dmp2, particularly under stressful conditions. Supporting this idea, we detected α-rings lacking α4 in Δ*dmp1* cells but not in wild-type cells. Thus, we propose that the Dmp1–Dmp2 complex acts as a chaperone for α-ring formation (**Fig. 4e**). This complex may inhibit inappropriate binding between α3 and α5. It may also accelerate the incorporation of α4 into the α-ring. Lastly, Dmp1–Dmp2 may ensure proper β-ring assembly by masking specific docking sites on the β subunits (**Fig. 6d**) to help locate the β2 subunit at its proper position on the α-ring.

Is the function mediated by Dmp1–Dmp2 conserved in eukaryotes other than budding yeast? PAC3 shares many characteristics with Dmp1–Dmp2. In PAC3-knockdown cells, α-ring formation is impaired, leading to decreased synthesis of 20S proteasomes[9]. Disruption of Dmp1 or Dmp2 also results in decreased formation of 20S proteasomes. Unfortunately, we did not detect α-rings using glycerol gradient fractionation even in wild-type yeast cells, possibly because the assembly of the 20S proteasome occurs more rapidly in yeast than in mammals. We did, however, identify α-rings lacking α4 in Δ*dmp1* cells by BN-PAGE and western blot analysis (**Fig. 4**), indicating that, as does PAC3, Dmp1–Dmp2 has a crucial role in α-ring formation. Another feature shared by Dmp1–Dmp2 and PAC3 is that they dissociate before the formation of half-proteasomes, as is often the case with chaperone molecules.

Consistent with the functional similarities described above, X-ray structural analysis revealed that Dmp1, Dmp2 and PAC3 share extensive structural similarities. Interestingly, the overall structure of Dmp1–Dmp2 resembles those of 20S proteasome α and β subunits, although the two β-sheets in the α and β subunits are made up of five β-strands[21,22] (**Supplementary Fig. 4** online). Attachment of β5 to α5 is achieved via interactions between H1 of β5 and H1, S3 and a loop between S2 and S3 of α5 (**Fig. 6a**, below). We initially predicted that the Dmp1–Dmp2 complex would interact with α5 in a similar manner. Structural analysis, however, revealed that the binding mode of Dmp1–Dmp2 to α5 is different from that of β5 to α5 (**Fig. 6a**). In the Dmp1–Dmp2–α-ring model, Dmp1–Dmp2 is located more deeply within the α-ring, which allows Dmp1–Dmp2 to interact with α4, α5 and α6, whereas β5 interacts with only α4 and α5 (**Fig. 6e**). The unique binding mode of Dmp1–Dmp2 may be essential for its role as a proteasome-assembling chaperone.

The crystal structure of Dmp1–Dmp2–α5 also provided important insights into the molecular mechanism underlying the release of Dmp1–Dmp2 from the precursor complex. Dmp1–Dmp2 does not attach to the α-ring in the presence of β4 because of steric hindrance between β4 and Dmp1 (**Fig. 6e,f**). This model is consistent with our *in vivo* immunoprecipitation data showing that, among the β subunits, only β2 was coimmunoprecipitated with Dmp1–Dmp2 (**Fig. 2b**). Although no interaction was observed between Dmp1–Dmp2 and the β subunits *in vitro*, PAC3 directly binds to several β subunits *in vitro*. It is possible that transient and/or weak interactions with these β subunits trigger the release of PAC3 from the proteasome precursors.

In conclusion, we have demonstrated that, regardless of whether Dmp1–Dmp2 and PAC3 are evolutionarily related (**Supplementary Discussion** and **Supplementary Figs. 5** and **6** online), chaperones are likely to contribute to 20S proteasome assembly in all eukaryotes. Such mechanisms presumably became important as the 20S proteasome increased its structural complexity by acquiring seven distinct subunits for each ring.

During the preparation of this manuscript, Poc3 and Poc4 were reported to be yeast 20S proteasome assembling chaperones, which are identical to Dmp2 and Dmp1, respectively[23].

METHODS

Strains and plasmids. The *E. coli* strain DH5α was used for propagating plasmids. BL21 (DE3) cells were used for expression and purification of recombinant proteins. Strain genotypes are given in **Supplementary Table 1** online. Yeast knockout strains (catalogue number YSC1053) were purchased from Open Biosystems. The plasmids used in this study are listed in **Supplementary Table 2** online.

Immunological analysis. SDS-PAGE, BN-PAGE and western blotting were carried out with the NuPAGE system (Invitrogen) as per instructions provided by the manufacturer. Anti-Dmp2, anti-HA (Babco), anti-Flag (Sigma), anti-ubiquitin (Chemicon), anti-Pgk1 (Molecular Probe), anti-20S[24] and anti-Rpn9 (ref. 25) antibodies were used at various points during the course of this study. Anti-Dmp2 was raised in rabbits using recombinant Dmp1–Dmp2 complex. 6×His-tagged Dmp1 and Dmp2 were coexpressed in *E. coli* and purified using Ni-affinity beads.

Table 1 Data collection, phasing and refinement statistics

	Dmp1,2 (Native)	Dmp1,2 (SeMet)			Dmp1,2 Δloop–α5	PAC3 (Native)	PAC3 (SeMet)
Data collection							
Space group	$P3_1$	$P6_322$			$P2_12_12$	$P4_32_12$	$P4_32_12$
Cell dimensions							
a, *b*, *c* (Å)	57.5, 57.5, 82.2	139.1, 139.1, 92.3			158.0, 158.5, 65.2	89.1, 89.1, 57.5	86.6, 86.6, 57.2
		Peak	*Inflection*	*Remote*			
Wavelength	0.9000	0.97925	0.97945	0.96408	0.9000	1.5418	1.5418
Resolution (Å)	1.96 (2.03–1.96)		3.60 (3.73–3.60)		2.90 (3.00–2.90)	2.00 (2.07–2.00)	1.80 (1.86–1.80)
R_{merge}	0.059 (0.187)	0.093 (0.518)	0.073 (0.433)	0.105 (0.551)	0.080 (0.350)	0.084 (0.452)	0.052 (0.479)
$I / \sigma I$	24.6	12.5	13.5	11.3	20.0	14.9	15.7
Completeness (%)	98.0 (93.7)	98.8 (94.9)	84.6 (85.2)	87.2 (87.1)	99.8 (99.9)	99.9 (99.9)	99.2 (98.1)
Redundancy	4.0 (2.6)	6.1 (4.8)	4.3 (3.7)	5.3 (4.7)	6.3 (6.4)	13.2 (12.4)	12.3 (10.8)
Refinement							
Resolution (Å)	49.8–1.96				50.4–2.90	27.5–2.00	
No. reflections	20,240						
R_{work} / R_{free}	0.240 / 0.287				0.250 / 0.283	0.180 / 0.252	
No. atoms							
Protein	2,079				6,604	1883	
Water	31				0	259	
B-factors (Å^2)							
Protein	40.9				66.9	24.8	
Water	37.6					35.8	
r.m.s. deviations							
Bond lengths (Å)	0.010				0.015	0.019	
Bond angles (°)	1.393				1.757	1.663	

Values in parentheses are for highest-resolution shell. One crystal was used for each data set. SeMet, selenomethionine-substituted protein.

Protein extraction. For immunoprecipitation and protein purification, cells were suspended in lysis buffer (50 mM HEPES-KOH (pH 7.6), 100 mM β-glycerolphosphate, 50 mM NaF, 1 mM $MgCl_2$, 1 mM EGTA, 5% (v/v) glycerol and 0.25% (v/v) Triton X-100 containing complete mini EDTA-free protease inhibitors (Roche)). For glycerol gradient analysis and BN-PAGE, cells were suspended in 50 mM HEPES-KOH (pH 7.6), 1 mM $MgCl_2$, 1 mM DTT and 2 mM ATP. Total cell lysates were prepared by vortexing with glass beads using a Multibeads shocker (Yasui Kikai) and cleared by centrifugation at 20,000 × *g* for 10 min at 4 °C.

Detection of polyubiquitinated proteins. Cells were suspended in 200 ml of cold ethanol containing 2 mM PMSF. Cells were lysed by agitation with 200 ml of glass beads for 10 min. Cells lysates were dried and suspended in sample buffer for western blotting. The primary antibody was anti-ubiquitin antibody (Chemicon), and the secondary antibody was anti-mouse IgG-horseradish peroxidase (Jackson ImmunoResearch).

Coimmunoprecipitation of tagged proteins. For **Figure 2e**, cell lysates from YT145 (Dmp1-3×Flag) and YT212 (Dmp1-3×Flag and Dmp2-3×HA) cells were mixed with anti-HA antibodies and incubated for 2 h, after which protein G–Sepharose beads (GE Healthcare) were added and the mixture was incubated for 1 h (left) or cell lysates from YT211 (Dmp2-3×HA) and YT212 (Dmp1-3×Flag and Dmp2-3×HA) were mixed with anti-Flag M2 agarose beads (Sigma) and incubated for 2 h. Then, immunoprecipitates were eluted in lysis buffer containing 200 μg ml^{-1} 3×Flag peptides (Sigma; right).

Glycerol gradient analysis. Cell extracts (2 mg of protein) were separated into 32 fractions by centrifugation (22 h, 100,000 × *g*) in 8–32% (v/v) glycerol linear gradients as described previously[5].

Binding assay. *In vitro* labeling was carried out using the TNT T7 Quick for PCR DNA system (Promega) with ^{35}S-labeled methionine, according to the manufacturer's instructions. Recombinant GST–Dmp1–Dmp2 was expressed in *E. coli* and purified with glutathione-Sepharose beads. The GST–Dmp1–Dmp2–bound beads were added to the labeling mixture and incubated on ice for 1 h. The resulting products were washed with PBS containing 0.5% (v/v) Triton X-100 and eluted using 50 mM Tris-HCl (pH 8.0), 50 mM NaCl, 1 mM EDTA, 1 mM DTT and 10 mM glutathione. The eluates were separated by SDS-PAGE and visualized using autoradiography.

Assay of proteasome activity. Peptidase activity was measured using a fluorescent peptide substrate, succinyl-Leu-Leu-Val-Tyr-7-amino-4-methylcoumarin (Suc-LLVY-AMC), as described previously[5]. A low concentration of SDS (0.025% (w/v)) was used as an artificial activator of 20S proteasomes that are usually latent in cells.

Induction of Dmp2 by galactose. YT596 (*GAL1p-DMP2*, α6-HA) and YT597 (*GAL1p-DMP2*, Δ*dmp1*, α6-HA) cells were grown overnight in 1.5 ml of YPD medium and then cultured in 10 ml of YPG medium to induce the expression of *DMP2* under the *GAL1* promoter. After incubation for 4 h or 8 h, cells were harvested and total cell lysates were subjected to BN-PAGE and immunoblotting with anti-HA antibodies or SDS-PAGE and immunoblotting with anti-Dmp2 antibodies.

Crystallization and data collection. Protein expression and purification were carried out as described in the **Supplementary Methods**. Crystallization of the Dmp1–Dmp2 complex was performed using the hanging-drop vapor diffusion method after mixing 3 μl of protein solution (20 mg ml^{-1}) and 1 μl of reservoir solution containing 25 mM MES (pH 6.5), 50 mM KH_2PO_4 and 16% (w/v) PEG8000. The selenomethionine (SeMet) crystals were grown at 20 °C by mixing 2 μl of protein solution and 2 μl of reservoir solution containing 0.1 M HEPES (pH 7.0) and 4.1 M NaCl. The Dmp1–Dmp2 Δloop–α5 crystals were

prepared using 0.1 M Tris-HCl (pH 8.5), 8% (v/v) ethylene glycol and 12% (w/v) PEG8000. PAC3 was crystallized using the hanging-drop vapor diffusion method after mixing 2 μl of protein solution with 2 μl of reservoir solution containing 0.1 M Tris-HCl (pH 8.5), 0.2 M $MgCl_2$ and 30% (w/v) PEG4000. SeMet PAC3 was similarly crystallized except that the pH was adjusted to 9.1.

Diffraction data sets for wild-type and SeMet Dmp1–Dmp2 as well as Dmp1–Dmp2 Δloop–α5 were collected at 100 K on beamline BL44XU (SPring-8). The diffraction data for native PAC3 and the SeMet derivative were collected using a Rigaku FR-E X-ray generator and a Rigaku R-AXIS VII detector. Data processing and reduction were carried out with the DENZO/SCALEPACK[26]. The crystal forms of wild-type Dmp1–Dmp2, SeMet Dmp1–Dmp2, Dmp1–Dmp2 Δloop–α5 and PAC3 belong to the $P3_1$, $P6_322$, $P2_12_12$, and $P4_32_12$ space groups, respectively. Data collection, phasing and refinement statistics are summarized in **Table 1**.

Structure determination and refinement. The structure of the Dmp1–Dmp2 complex was determined using multiwavelength anomalous diffraction (MAD) and SeMet proteins. The positions of heavy atoms were obtained using SHELXD[27] and refined with SHARP[28]. Initial MAD phases were extended to 3.6 Å and improved with solvent flattening and histogram mapping using DM[29]. The structure of wild-type Dmp1–Dmp2 was determined by molecular replacement using MOLREP[30] with SeMet Dmp1–Dmp2 as a search model. An initial model was built using ARP/wARP[31]. Manual building was then carried out using the program COOT[32] and alternated with several cycles of refinement using the program REFMAC5 (ref. 33).

The structure of Dmp1–Dmp2 Δloop–α5 was determined using the molecular replacement technique MOLREP and the structures of Dmp1–Dmp2 and α5 (PDB ID code 1RYP). The PAC3 structure was solved using the single-wavelength anomalous diffraction (SAD) method and the programs SHELXD and SHARP. Phasing and refinement statistics are summarized in **Table 1**. There are no residues in disallowed regions of the Ramachandran plot. Structure figures were generated using MOLSCRIPT[34], RASTER3D[35], and CCP4MG[36].

Accession codes. Protein Data Bank: Coordinates have been deposited under accession numbers 2Z5B for Dmp1–Dmp2, 2Z5C for Dmp1–Dmp2–α5 and 2Z5E for PAC3.

Note: Supplementary information is available on the Nature Structural & Molecular Biology website.

ACKNOWLEDGMENTS

We thank all of the members of BL44XU, especially E. Yamashita and M. Yoshimura, for their help in data collection at SPring-8 and T. Hikage for his help in X-ray diffraction data collection for PAC3. This work was supported by grants from Japan Science and Technology Agency (to S.M.), the Ministry of Education, Culture, Sports, Science and Technology (MEXT) of Japan (to H.Y., T.M., S.M., E.K., K.K. and K. Tanaka) and the Target Protein Project of MEXT (to T.M., K.K. and K. Tanaka and the Takeda Science Foundation (to K. Tanaka)). E.S. is a recipient of a Japan Society for the Promotion of Science Research Fellowship for Young Scientists.

AUTHOR CONTRIBUTIONS

H.Y. and T. Kameyama performed all of the yeast experiments. T.M., H.Y., K. Takagi and T.Y. determined the structures of the Dmp1–Dmp2 and Dmp1–Dmp2 Δloop-α5 complexes. K.O., E.K., E.S., A.S., Y.H., S.M., T.Y. and K.K. determined the structure of PAC3. H.H., T. Kishimoto and S.N. conducted the mass spectrometric analysis. M.K. performed phylogenetic analyses. H.Y., T.M., K.K., M.K. and K. Tanaka wrote the paper. All of the authors discussed the results and commented on the manuscript.

Published online at http://www.nature.com/nsmb/
Reprints and permissions information is available online at http://npg.nature.com/reprintsandpermissions

1. Baumeister, W., Walz, J., Zuhl, F. & Seemuller, E. The proteasome: paradigm of a self-compartmentalizing protease. *Cell* **92**, 367–380 (1998).
2. Coux, O., Tanaka, K. & Goldberg, A.L. Structure and functions of the 20S and 26S proteasomes. *Annu. Rev. Biochem.* **65**, 801–847 (1996).
3. Zwickl, P., Kleinz, J. & Baumeister, W. Critical elements in proteasome assembly. *Nat. Struct. Biol.* **1**, 765–770 (1994).
4. Chen, P. & Hochstrasser, M. Biogenesis, structure and function of the yeast 20S proteasome. *EMBO J.* **14**, 2620–2630 (1995).
5. Hirano, Y. *et al.* A heterodimeric complex that promotes the assembly of mammalian 20S proteasomes. *Nature* **437**, 1381–1385 (2005).
6. Nandi, D., Woodward, E., Ginsburg, D.B. & Monaco, J.J. Intermediates in the formation of mouse 20S proteasomes: implications for the assembly of precursor β subunits. *EMBO J.* **16**, 5363–5375 (1997).
7. Li, X., Kusmierczyk, A.R., Wong, P., Emili, A. & Hochstrasser, M. β-Subunit appendages promote 20S proteasome assembly by overcoming an Ump1-dependent checkpoint. *EMBO J.* **26**, 2339–2349 (2007).
8. Ramos, P.C., Hockendorff, J., Johnson, E.S., Varshavsky, A. & Dohmen, R.J. Ump1p is required for proper maturation of the 20S proteasome and becomes its substrate upon completion of the assembly. *Cell* **92**, 489–499 (1998).
9. Hirano, Y. *et al.* Cooperation of multiple chaperones required for the assembly of mammalian 20S proteasomes. *Mol. Cell* **24**, 977–984 (2006).
10. Burri, L. *et al.* Identification and characterization of a mammalian protein interacting with 20S proteasome precursors. *Proc. Natl. Acad. Sci. USA* **97**, 10348–10353 (2000).
11. Heink, S., Ludwig, D., Kloetzel, P.M. & Kruger, E. IFN-γ-induced immune adaptation of the proteasome system is an accelerated and transient response. *Proc. Natl. Acad. Sci. USA* **102**, 9241–9246 (2005).
12. Jayarapu, K. & Griffin, T.A. Protein-protein interactions among human 20S proteasome subunits and proteassemblin. *Biochem. Biophys. Res. Commun.* **314**, 523–528 (2004).
13. Bachmair, A., Finley, D. & Varshavsky, A. *In vivo* half-life of a protein is a function of its amino-terminal residue. *Science* **234**, 179–186 (1986).
14. Johnson, E.S., Ma, P.C., Ota, I.M. & Varshavsky, A. A proteolytic pathway that recognizes ubiquitin as a degradation signal. *J. Biol. Chem.* **270**, 17442–17456 (1995).
15. Meimoun, A. *et al.* Degradation of the transcription factor Gcn4 requires the kinase Pho85 and the SCF(CDC4) ubiquitin-ligase complex. *Mol. Biol. Cell* **11**, 915–927 (2000).
16. Mannhaupt, G., Schnall, R., Karpov, V., Vetter, I. & Feldmann, H. Rpn4p acts as a transcription factor by binding to PACE, a nonamer box found upstream of 26S proteasomal and other genes in yeast. *FEBS Lett.* **450**, 27–34 (1999).
17. Xie, Y. & Varshavsky, A. RPN4 is a ligand, substrate, and transcriptional regulator of the 26S proteasome: a negative feedback circuit. *Proc. Natl. Acad. Sci. USA* **98**, 3056–3061 (2001).
18. Glickman, M.H. *et al.* Functional analysis of the proteasome regulatory particle. *Mol. Biol. Rep.* **26**, 21–28 (1999).
19. Fehlker, M., Wendler, P., Lehmann, A. & Enenkel, C. Blm3 is part of nascent proteasomes and is involved in a late stage of nuclear proteasome assembly. *EMBO Rep.* **4**, 959–963 (2003).
20. Schmidt, M. *et al.* The HEAT repeat protein Blm10 regulates the yeast proteasome by capping the core particle. *Nat. Struct. Mol. Biol.* **12**, 294–303 (2005).
21. Groll, M. *et al.* Structure of 20S proteasome from yeast at 2.4 Å resolution. *Nature* **386**, 463–471 (1997).
22. Unno, M. *et al.* The structure of the mammalian 20S proteasome at 2.75 Å resolution. *Structure* **10**, 609–618 (2002).
23. Tallec, B. *et al.* 20S Proteasome assembly is orchestrated by two distinct pairs of chaperones in yeast and in mammals. *Mol. Cell* **27**, 660–674 (2007).
24. Tanaka, K. *et al.* Proteasomes (multi-protease complexes) as 20 S ring-shaped particles in a variety of eukaryotic cells. *J. Biol. Chem.* **263**, 16209–16217 (1988).
25. Takeuchi, J., Fujimuro, M., Yokosawa, H., Tanaka, K. & Toh-e, A. Rpn9 is required for efficient assembly of the yeast 26S proteasome. *Mol. Cell. Biol.* **19**, 6575–6584 (1999).
26. Otwinowski, Z. & Minor, W. Processing of x-ray diffraction data collected in oscillation mode. *Methods Enzymol.* **276**, 307–326 (1997).
27. Schneider, T.R. & Sheldrick, G.M. Substructure solution with SHELXD. *Acta Crystallogr. D Biol. Crystallogr.* **58**, 1772–1779 (2002).
28. Bricogne, G., Vonrhein, C., Flensburg, C., Schiltz, M. & Paciorek, W. Generation, representation and flow of phase information in structure determination: recent developments in and around SHARP 2.0. *Acta Crystallogr. D Biol. Crystallogr.* **59**, 2023–2030 (2003).
29. CCP4. The CCP4 suite: programs for protein crystallography. *Acta Crystallogr. D Biol. Crystallogr.* **50**, 760–763 (1994).
30. Vagin, A.A. & Teplyakov, A. MOLREP: an automated Program for molecular replacement. *J. Appl. Crystallogr.* **30**, 1022–1025 (1997).
31. Morris, R.J., Perrakis, A. & Lamzin, V.S. ARP/wARP and automatic interpretation of protein electron density maps. *Methods Enzymol.* **374**, 229–244 (2003).
32. Emsley, P. & Cowtan, K. Coot: model-building tools for molecular graphics. *Acta Crystallogr. D Biol. Crystallogr.* **60**, 2126–2132 (2004).
33. Murshudov, G.N., Vagin, A.A. & Dodson, E.J. Refinement of macromolecular structures by the maximum-likelihood method. *Acta Crystallogr. D Biol. Crystallogr.* **53**, 240–255 (1997).
34. Kraulis, P.J. MOLSCRIPT: a program to produce both detailed and schematic plots of protein structures. *J. Appl. Crystallogr.* **24**, 946–950 (1991).
35. Merritt, E.A. & Murphy, M.E. Raster3D Version 2.0. A program for photorealistic molecular graphics. *Acta Crystallogr. D Biol. Crystallogr.* **50**, 869–873 (1994).
36. Potterton, E., McNicholas, S., Krissinel, E., Cowtan, K. & Noble, M. The CCP4 molecular-
graphics project. *Acta Crystallogr. D Biol. Crystallogr.* **58**, 1955–1957 (2002).

The EMBO Journal (2008) 27, 2204–2213 | © 2008 European Molecular Biology Organization | All Rights Reserved 0261-4189/08
www.embojournal.org

THE EMBO JOURNAL

Dissecting β-ring assembly pathway of the mammalian 20S proteasome

Yuko Hirano[1], Takeumi Kaneko[2], Kenta Okamoto[3], Minghui Bai[2], Hideki Yashiroda[2], Kaori Furuyama[2], Koichi Kato[3,4], Keiji Tanaka[1] and Shigeo Murata[2,*]

[1]Laboratory of Frontier Science, Tokyo Metropolitan Institute of Medical Science, Tokyo, Japan, [2]Laboratory of Protein Metabolism, Department of Integrated Biology, Graduate School of Pharmaceutical Sciences, The University of Tokyo, Tokyo, Japan, [3]Department of Structural Biology and Biomolecular Engineering, Graduate School of Pharmaceutical Sciences, Nagoya City University, Nagoya, Japan and [4]Division of Biomolecular Functions, Department of Life and Coordination-Complex Molecular Science, Institute for Molecular Science, National Institutes of Natural Sciences, Okazaki, Japan

The 20S proteasome is the catalytic core of the 26S proteasome. It comprises four stacked rings of seven subunits each, $\alpha_{1-7}\beta_{1-7}\beta_{1-7}\alpha_{1-7}$. Recent studies indicated that proteasome-specific chaperones and β-subunit appendages assist in the formation of α-rings and dimerization of half-proteasomes, but the process involved in the assembly of β-rings is poorly understood. Here, we clarify the mechanism of β-ring formation on α-rings by characterizing assembly intermediates accumulated in cells depleted of each β-subunit. Starting from β2, incorporation of β-subunits occurs in an orderly manner dependent on the propeptides of β2 and β5, and the C-terminal tail of β2. Unexpectedly, hUmp1, a chaperone functioning at the final assembly step, is incorporated as early as β2 and is required for the structural integrity of early assembly intermediates. We propose a model in which β-ring formation is assisted by both intramolecular and extrinsic chaperones, whose roles are partially different between yeast and mammals.

The EMBO Journal (2008) **27**, 2204–2213. doi:10.1038/emboj.2008.148; Published online 24 July 2008
Subject Categories: proteins
Keywords: assembly; chaperone; propeptide; proteasome; ubiquitin

Introduction

The ubiquitin–proteasome system is the main pathway for ATP-dependent non-lysosomal degradation of intracellular proteins in eukaryotes (Coux *et al*, 1996; Baumeister *et al*, 1998). Protein degradation achieved by this system is involved in various cellular processes, including cell cycle regulation, stress response, intracellular signalling, transcription regulation, and acquired immunity (Glickman and Ciechanover, 2002). Proteins involved in such regulatory processes as well as damaged proteins are recognized by the ubiquitin system and are marked for degradation by covalent attachment of polyubiquitin chains. Polyubiquitinated proteins are then recognized and degraded by the 26S proteasome, a 2.5-MDa multisubunit protease.

The 26S proteasome is composed of a catalytic core particle, called the 20S proteasome, bound at one or both ends by a 19S regulatory particle. The 20S proteasome is a cylindrical structure comprised of 28 subunits arranged in four stacked seven-membered rings. Each ring contains seven different subunits, whereby the two outer rings are formed by non-catalytic α-type subunits, named α1–α7, and the two inner rings are formed by the β-type subunits, β1–β7, three of which are catalytic (β1, β2, and β5) (Baumeister *et al*, 1998). Each of the 14 different proteins occupies a defined position within the 20S proteasome (Groll *et al*, 1997; Unno *et al*, 2002). Vertebrates encode four additional catalytic β-subunits; three interferon-γ-inducible β1i, β2i, and β5i and one thymus-specific β5t, which are incorporated in place of their most closely related β-subunits, thus forming distinct subtypes of proteasomes with altered catalytic activities called immunoproteasome and thymoproteasome (Tanaka and Kasahara, 1998; Murata *et al*, 2007).

The integrity of the 20S proteasome is assured by correct assembly of the 14 α-subunits and 14 β-subunits. All of the active β-subunits as well as non-catalytic β6 and β7 are synthesized with N-terminal propeptides, which are removed autocatalytically at the final step of the assembly to expose the catalytic threonine residues of β1, β2, and β5. The N-terminal active sites of β-subunits are on the inner surface of the β-rings, whereas the C termini of β-subunits are on the outer surface of the 20S proteasome (Groll *et al*, 1997). It has been shown that efficient assembly of the 20S proteasome is orchestrated by proteasome-specific chaperones such as PAC1 (Pba1 or POC1 in yeast), PAC2 (Pba2 or POC2 in yeast), PAC3 (Pba3, Dmp2, or POC3 in yeast), PAC4 (Pba4, Dmp1, or POC4 in yeast), hUmp1 (also known as POMP, proteassemblin in mammals and as Ump1 in yeast), the N-terminal propeptides of β-subunits, and C-terminal tails of β-subunits, which provide specific subunit interactions with *cis*- and *trans*-β-rings (Heinemeyer *et al*, 2004; Ramos *et al*, 2004; Hirano *et al*, 2005, 2006; Murata, 2006; Le Tallec *et al*, 2007; Li *et al*, 2007; Kusmierczyk *et al*, 2008; Yashiroda *et al*, 2008).

Proteasome assembly proceeds through distinct assembly intermediates. The earliest intermediate observed in mammalian cells is an α-ring that is comprised of all seven α-subunits, a PAC1–PAC2 heterodimer, and a PAC3–PAC4 complex (Hirano *et al*, 2005, 2006; Le Tallec *et al*, 2007). Both PAC1–PAC2 and PAC3–PAC4 are involved in the

*Corresponding author. Laboratory of Protein Metabolism, Department of Integrated Biology, Graduate School of Pharmaceutical Sciences, The University of Tokyo, 7-3-1 Hongo, Bunkyo-ku, Tokyo 113-0033, Japan. Tel.: +81 3 5841 4803; Fax: +81 3 5841 4805;
E-mail: smurata@mol.f.u-tokyo.ac.jp

Received: 14 April 2008; accepted: 3 July 2008; published online: 24 July 2008

formation of α-rings. Recently, Pba3–Pba4 or Dmp1–Dmp2, yeast orthologues of PAC3–PAC4, has shown to catalyse correct subunit orientation of an α-ring (Kusmierczyk *et al*, 2008; Yashiroda *et al*, 2008). PAC1–PAC2 prevents non-productive dimerization of α-rings. The α-ring serves as a scaffold for the assembly of β-subunits. Another intermediate is the 13S complex composed of one α-ring, unprocessed β2, β3, β4, and (h)Ump1, both in yeast and mammals (Frentzel *et al*, 1994; Nandi *et al*, 1997; Li *et al*, 2007). Recent studies in yeast showed that the addition of the other β-subunits except β7 form the subsequent intermediate referred to as a 'half-mer' precursor complex (Li *et al*, 2007; Marques *et al*, 2007). The 16S complex containing all the subunits and hUmp1 has been described also in mammalian cells (Schmidtke *et al*, 1997; Witt *et al*, 2000). A 'half-proteasome' is often used as a general term for assembly intermediates containing unprocessed β-subunits and (h)Ump1. Studies in yeast have shown that dimerization of the half-mer is driven by the propeptide of β5 and the C-terminal tail of β7, whose incorporation into the half-proteasome is coupled with the dimerization, where the role of Ump1 is proposed to be an assembly checkpoint factor that inhibits the dimerization until a full set of β-subunits are recruited on the α-ring (Ramos *et al*, 2004; Li *et al*, 2007). Removal of β-propeptides and degradation of Ump1 coincide with completion of proteasome maturation, followed by degradation of PAC1–PAC2 (Ramos *et al*, 1998; Hirano *et al*, 2005). PAC3 is released from the intermediates during the maturation process (Hirano *et al*, 2006).

Several studies in yeast reported that the propeptides and the C-terminal tails of certain β-subunits have important roles in proteasome biogenesis. The propeptide of β5 is crucial for the incorporation of β5 during proteasome formation and is thus essential for life (Chen and Hochstrasser, 1996). The propeptides of β1 and β2 are dispensable for cell viability but are known to protect the N-terminal catalytic threonine residue against N^{α}-acetylation. In addition, mutants lacking these two propeptides displayed modest defects in proteasome biogenesis (Arendt and Hochstrasser, 1999). The C-terminal tail of β2, which wraps around β3 within the same β-ring, is also essential for proteasome biogenesis in yeast (Groll *et al*, 1997; Ramos *et al*, 2004). The C-terminal tail of β7, which is inserted into a groove between β1 and β2 in the opposite ring, also has an important function in dimerization of half-proteasomes as well as stabilization of active conformation of β1 (Groll *et al*, 1997; Ramos *et al*, 2004). In mammals, analysis of propeptides has been mainly conducted in the context of immunoproteasome formation, but there is little or no information on the C-terminal tails of β2 and β7, whose location in the mammalian proteasome closely resembles those of yeast β2 and β7 in the yeast proteasome (Unno *et al*, 2002).

Here, we describe a series of biochemical experiments employing RNA interference of each β-subunit, which resulted in the accumulation of distinct assembly intermediates. By characterizing these intermediates, we clarified the order of β-subunit incorporation on the α-ring. We also assessed the roles of propeptides and C-terminal tails of β-subunits in mammalian proteasome biogenesis, which revealed that these appendages mostly function in a manner similar to yeast counterparts but also displayed some phenotypes not observed in yeast. Furthermore, we identified a novel function of hUmp1 in stabilizing assembly intermediate of proteasomes that has not been appreciated in yeast.

Results

Ordered assembly of β-subunits on α-ring

During the assembly pathway from the α-ring through the half-proteasome, each β-subunit assembles on the α-ring. To clarify the order of incorporation of β-subunits, we used the strategy of small interfering RNA (siRNA)-mediated knockdown of each β-subunit, which was expected to result in arrest of the assembly process before the incorporation of the targeted subunit and accumulation of a specific intermediate.

The total level of the different subunits as well as proteasome activity assessed by the peptide-hydrolysing activity of HEK293T cells transfected with siRNA targeting each β-subunit or hUmp1 was markedly reduced compared with those of control cells, suggesting that the biogenesis of proteasomes is severely impaired in each knockdown cell (Supplementary Figure S1). Each cell extract was resolved by native PAGE, followed by active staining or immunoblot analyses for α6- and all β-subunits (Figure 1). Immunoblot for α6 revealed accumulation of different complexes (molecular weight, 232–669 kDa) in each knockdown cell, as well as the normal α-ring in control cells, which have been shown to be a distinct assembly intermediate comprising all the seven α-subunits, PAC1–PAC2, and PAC3 (Hirano *et al*, 2006) (Figure 1A). Besides the major, fast-migrating band, a more slowly migrating minor band was observed for each knockdown cell except β2, β3, and hUmp1 knockdown (Figure 1A). Both the major and minor species did not show any peptide-hydrolysing activity, which was observed only in the complex of approximately 700-kDa, that is, 20S proteasomes (Figure 1B), indicating that they are assembly intermediates of 20S proteasomes.

Among the seven β-subunits, β2 was the first assembled on the α-ring based on the finding that β2 was detected in all the intermediates except for that in its own knockdown (Figure 1D) and the intermediate that accumulated in β2-knockdown cells did not contain any β-subunit (Figure 1C–I, lanes for β2 RNAi). The assembly of β3 followed that of β2; β3 was detected in the intermediates observed in β1-, β4-, β5-, β6-, and β7-knockdown cells, and thus the incorporation of β3 should precede these subunits (Figure 1E). This view was further confirmed by the fact that the intermediate in β3-knockdown cells contained only β2 among the β-subunits (Figure 1C–I, lanes for β3 RNAi). β3 assembly was followed by β4 incorporation, which would result in the formation of the 13S complex, comprising the α-ring plus β2, β3, and β4, as suggested by the presence of β4 in the intermediate in β1, β5, β6, and β7 knockdown (Figure 1F), consistent with the previous reports that identified the 13S complex as a distinct entity of proteasome precursors (Frentzel *et al*, 1994; Nandi *et al*, 1997; Li *et al*, 2007).

β5 was the next β-subunit incorporated into the 13S complex because β5 was detected only in the intermediates in β1-, β6-, and β7-knockdown cells (Figure 1G). The assembly of β6 followed that of β5, as evidenced by the presence of β6 in the intermediates of β1 and β7 knockdown

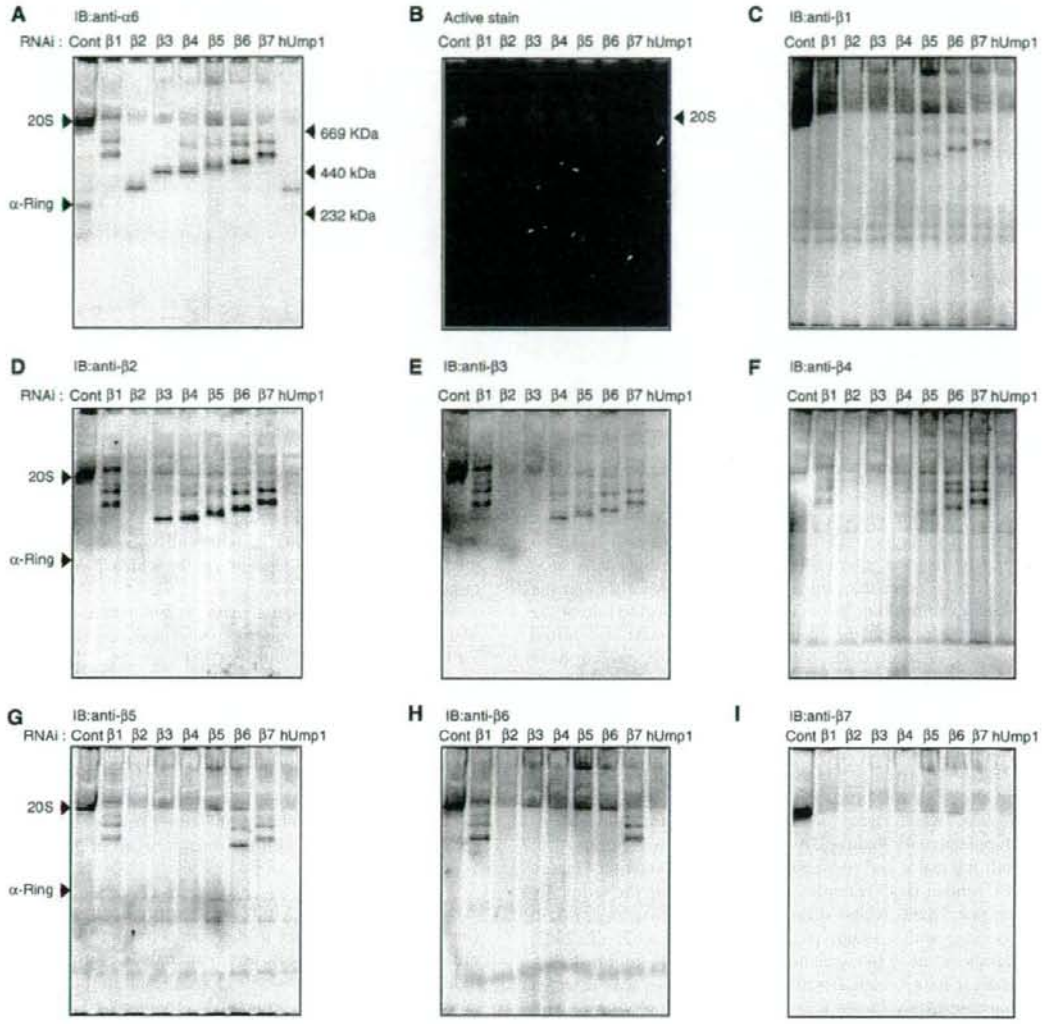

Figure 1 Accumulation of distinct assembly intermediates in each β-subunit knockdown cells. The cell extracts (40 μg) used in Supplementary Figure S1 were separated by native PAGE. Assembly intermediates were detected by immunoblotting using the indicated antibodies (**A**, **C**–**I**) The bands corresponding to α-ring and the 20S proteasome as well as the locations of molecular size markers are depicted by arrowheads. (**B**) The peptide-hydrolysing activity was assayed by active staining of the gel using Suc-LLVY-MCA in the presence of SDS. Note that the 26S proteasome did not move inside the native PAGE gel.

(Figure 1H). β7 was likely the last β-subunit incorporated in the precursor proteasomes because β7 was not found in any of the intermediate complexes (Figure 1I) and because the intermediate observed in β7-knockdown cells contained all the β-subunits with the exception of β7 (Figure 1C–I, lanes for β7 RNAi). The behaviour of β1 was rather elusive. The intermediate in β1-knockdown cells contained β2, β3, β4, β5, and β6 (Figure 1C–I, lanes for β1 RNAi), whereas β1 was already included in the intermediates of β4, β5, β6, and β7 knockdown (Figure 1C). The former observation suggests that β1 was incorporated following β2, β3, β4, β5, and β6, and that β1 is required for β7 incorporation. The latter observation suggests that the presence of β2 and β3 is sufficient for the incorporation of β1 and that β1 can be incorporated anytime during the maturation pathway from the complex containing both β2 and β3 through the half-mer.

Association of PA28, Hsp90, and Hsc70 with 20S proteasome precursors

When the same panel was probed for PAC1, the major assembly intermediate bands were associated with PAC1 (Figure 2A), which has been shown to be retained in the proteasome precursor until the completion of the assembly

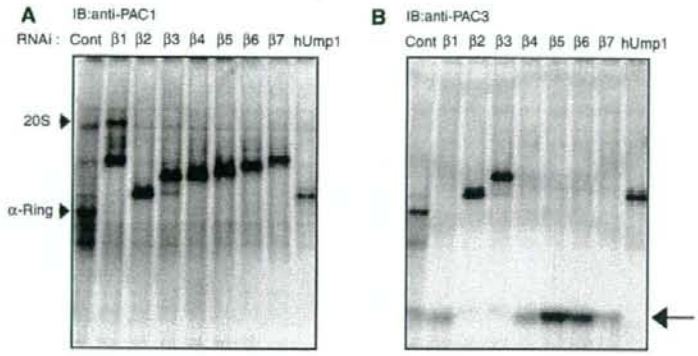

Figure 2 Release of PAC3 is coupled with β3 incorporation. The same panels in Figure 1 were probed with anti-PAC1 (**A**) and -PAC3 (**B**) antibodies. The arrow indicates PAC3 species dissociated from proteasome precursors (B).

(Hirano *et al*, 2005). However, the slowly migrating minor bands above the major bands did not contain PAC1, whereas the composition of each major and minor bands in terms of α- and β-subunits is identical (Figures 1 and 2A). It is also curious that the intermediate in β2-knockdown cells was apparently larger than the α-ring (Figure 1A), although the subunit composition is supposed to be identical to that of the α-ring. To address the identity of these bands, we tested whether PA28, PA200, Hsp90α, and Hsc70, which have been reported to be involved in proteasome biogenesis (Schmidtke *et al*, 1997; Preckel *et al*, 1999; Fehlker *et al*, 2003; Imai *et al*, 2003; Marques *et al*, 2007), associate with the intermediates.

PA28 was associated with the slow-migrating minor bands but not with the primary bands, different from PAC1 and Hsp90α, which were detected only in the major bands (Supplementary Figure S2A and B). Hsc70 was observed in both the major and the minor bands (Supplementary Figure 2C). Neither Hsp90α nor Hsc70 was detected in the α-ring. By contrast, PA200, whose yeast orthologue Blm10 was shown to associate with nascent proteasomes (Fehlker *et al*, 2003; Marques *et al*, 2007), was not observed in the intermediates, whereas its association with 20S proteasomes was detected (Supplementary Figure S2D, arrowhead). However, we cannot conclude that PA200 is not bound to assembly intermediates as free forms of PA200, which probably dissociated from 20S or nascent proteasomes during native PAGE analysis, were found (Supplementary Figure S2D, arrow).

The association of Hsp90 and Hsc70 with the assembly intermediates accounts for the increased size of the intermediate in β2-knockdown cells and suggests that recruitment of these chaperones precedes β2 and hUmp1 incorporation. The minor bands are characterized by the association of PA28, a 200-kDa heterohexameric complex. At present, we do not know whether these molecules really have some functions in the proteasome biogenesis or are associated with the intermediates as an experimental artefact. Further studies are needed to answer this question.

Release of PAC3 upon incorporation of β3

We previously showed that precursor proteasomes purified with tagged hUmp1 did not contain PAC3 and demonstrated that PAC3 is released during the maturation pathway of the mammalian proteasome (Hirano *et al*, 2006). To elucidate the step where PAC3 was released, we took advantage of the knockdown experiments in which distinct assembly intermediates accumulated depending on which β-subunit was targeted (Figure 1).

The same panel in Figure 1 was probed with anti-PAC1 and -PAC3 antibody. All the assembly intermediates as well as the α-ring were associated with PAC1 (Figure 2A) (Hirano *et al*, 2005). PAC3 is also associated with the α-ring in control cells as reported previously (Hirano *et al*, 2006). However, PAC3 was associated with intermediates of β2-, β3-, and hUmp1-knockdown cells but not with those of others, where PAC3 was found as fast migrating species, presumably as a free complex (Figure 2B, arrow). Considering the order of incorporation of β-subunits shown in Figure 1, the release of PAC3 is apparently coupled with the incorporation of β3.

A new role of hUmp1 in the assembly pathway

One intriguing difference in the phenotypes of loss of Ump1 orthologues between yeast and mammals is that knockdown of hUmp1 in mammalian cells did not result in the accumulation of intermediates containing unprocessed β-subunits (Figure 1, lanes for hUmp1 RNAi), whereas deletion of Ump1 in yeast caused apparent accumulation of such intermediates (Ramos *et al*, 1998). This observation in hUmp1-knockdown cells has also been shown in previous studies (Hirano *et al*, 2005, 2006). This finding raises the possibility that the role of Ump1 orthologues is different between yeast and mammals.

To determine the step at which hUmp1 is incorporated, the same panel in Figure 1 was probed with anti-hUmp1 antibody. hUmp1 was included in a complex other than that in β2-knockdown cells (Figure 3A), indicating that the incorporation of hUmp1 precedes that of β3. On the other hand, the intermediate in the hUmp1 knockdown complex did not contain any of the β-subunits, including β2, a finding closely resembling that in β2-knockdown cells with regard to size and composition (Figures 1 and 2; compare lanes for β2 RNAi to lanes for hUmp1 RNAi). These results suggest that incorporations of β2 and hUmp1 are coupled with each other and that loss of either result in dissociation of the other.

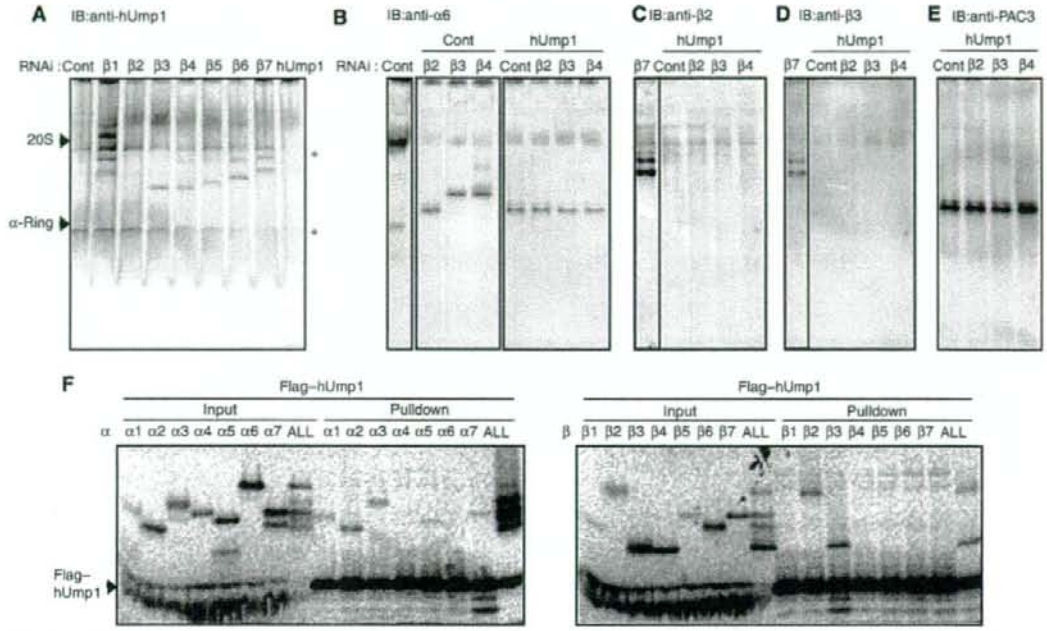

Figure 3 Role of hUmp1 in the structural integrity of early assembly intermediates. (**A**) The same panel in Figure 1 was probed with anti-hUmp1 antibody. (**B–E**) Extracts of HEK293T cells transfected with the indicated combinations of siRNAs were separated by native PAGE. Intermediate complexes were detected by immunoblotting using the indicated antibodies. The left lane representing β7 RNAi serves as a positive control for immunoblotting (C, D). Asterisks indicate nonspecific bands (A). (**F**) Flag–hUmp1 and each 20S subunit were co-translated and radio-labelled in reticulocyte lysates, immunoprecipitated with M2 agarose, and analysed by SDS–PAGE and autoradiography. 'ALL' represents co-translation of all β-subunits together with hUmp1.

To confirm this concept, hUmp1 was knocked down concurrently with β2, β3, or β4, and the resultant assembly intermediates were compared with those in β2, β3, or β4 single-knockdown cells. Intriguingly, the size of intermediates observed in the simultaneous knockdown of hUmp1 with β3 or β4 was similar to that of the complex in β2 single-knockdown cells (Figure 3B). Notably, the intermediate found in β3–hUmp1 double-knockdown cells lacked β2 (Figure 3C), which was found in the complex of β3 single-knockdown cells (Figure 1D). The β4 and hUmp1 double knockdown was associated with loss of both β2 and β3 in the intermediate (Figure 3C and D), which were clearly detected in the β4 single knockdown complex (Figure 1D and E). Furthermore, the complexes manifested in the double knockdown cells were associated with PAC3, consistent with the absence of β3, whose incorporation would detach PAC3 from the precursor proteasome (Figures 2B and 3E).

To gain mechanistic insight into the early function of hUmp1, we tested the interactions between hUmp1 and each 20S proteasome subunit. hUmp1 could directly bind to β2 and β3 as well as some of the α-subunits (α2, α3, α5, and α7) (Figure 3F). This observation raises the possibility that hUmp1, either alone or as a complex with β2 and β3, is recruited on the α-ring through direct interaction between hUmp1 and certain α-subunits.

Taken together, these results demonstrate that β2 is unable to associate with the α-ring without hUmp1 and suggest the important role of hUmp1 in promoting the maturation process beyond the α-ring, either by stabilizing the complex or by recruiting β2.

Propeptides of β1, β6, and β7 are dispensable for proteasome maturation

It has been reported that the propeptides and C-terminal tails of β-subunits have important roles in proteasome biogenesis in yeast (Chen and Hochstrasser, 1996; Ramos *et al*, 2004; Li *et al*, 2007; Marques *et al*, 2007), but little is known about their roles in the maturation of proteasomes in mammals.

To elucidate the role of propeptides of β1, β2, β5, β6, and β7, and the C-terminal tails of β2 and β7 in mammals, we first established cell lines stably transfected with constructs encoding wild-type subunits (β1*, β2*, β5*, β6*, and β7*), mature subunits whose propeptides were replaced with ubiquitin (β1*Δpro, β2*Δpro, β5*Δpro, β6*Δpro, and β7*Δpro), and β2 and β7 lacking their C-terminal tails (β2*Δtail and β7*Δtail) (Supplementary Figure S3A). Synonymous mutations were introduced into these constructs so that they were not sensitive to siRNAs against each β-subunit used in Figure 1. These constructs were attached with C-terminal Flag tag to distinguish the expressed proteins from endogenous proteins. We first confirmed the expression of both precursor and mature forms of β-subunits in HEK293T cells transfected with constructs encoding wild-type and Δtail β-subunits (Supplementary Figure S3B). On the other hand, as expected, only mature forms of β-subunits were detected in cells transfected with ubiquitin-fused Δpro constructs

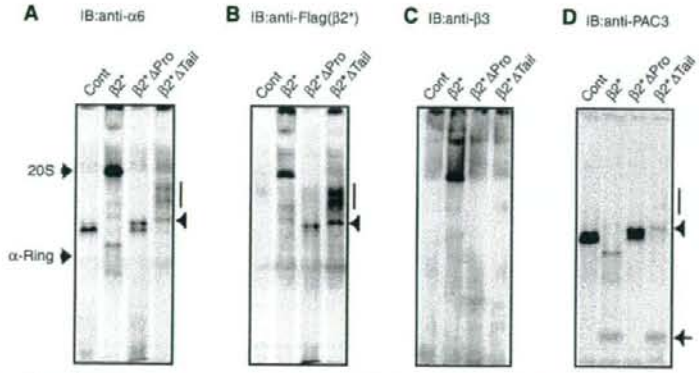

Figure 4 Both the propeptide and C-terminal tail of β2 are indispensable for β3 incorporation. Stable cell lines expressing the indicated mutant β2-subunits were treated with the siRNA targeting endogenous β2. Intermediate complexes were detected by immunoblotting using the indicated antibodies following native PAGE (**A–D**). Intermediates observed in β2*ΔTail cells can be divided into two species; faster migrating ones (arrowheads) and slower migrating ones (vertical bars). The free complex of PAC3 is depicted by an arrow (D).

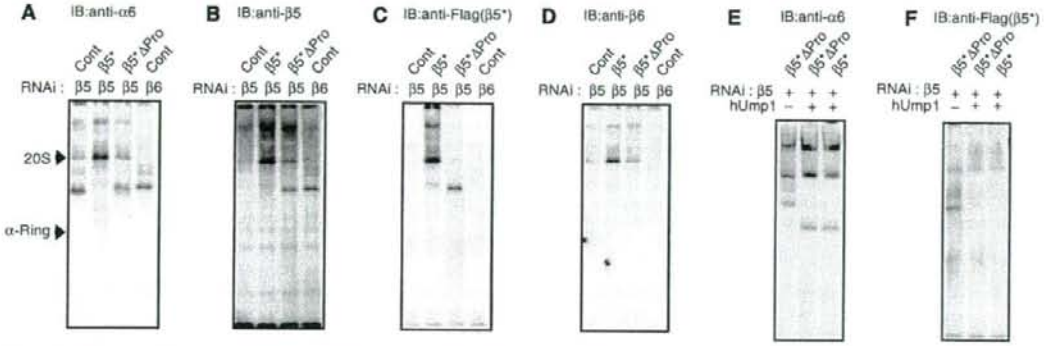

Figure 5 β5 propeptide is required for β6 incorporation. Stable cell lines expressing the indicated mutant β5-subunits were treated with the siRNA(s) for endogenous β5 or β6 (**A–D**), or for the indicated combinations (**E, F**). Cell extracts were resolved by native PAGE, followed by immunoblot analysis for the indicated antibodies.

(Supplementary Figure S3B). These ubiquitin-fused proteins are known to be cleaved rapidly by cellular deubiquitinating enzymes to generate free ubiquitin and the mature moiety of the proteasome subunit, so that the exposure and integrity of the N-terminal residue are ensured (Chen and Hochstrasser, 1996; Arendt and Hochstrasser, 1999; Jager *et al*, 1999). siRNA-mediated knockdown of endogenous subunits in these cells allowed us to determine the precise roles of propeptides and C-terminal tails.

Expression of constructs encoding each wild-type subunit (β1*, β2*, β5*, β6*, and β7*) restored production of 20S proteasomes and rescued cells from death caused by siRNA treatment (data not shown), verifying that exogenously expressed constructs worked appropriately (Figures 4A, 5A and 6A; Supplementary Figures S4 and S5). Among the Δpro constructs, cells expressing β1*Δpro, β6*Δpro, and β7*Δpro grew apparently normal and produced 20S proteasomes at an amount comparable to wild-type expressing cells (Supplementary Figures S4 and S5; Figure 6A). These findings indicate that the propeptides of β1, β6, and β7 are not

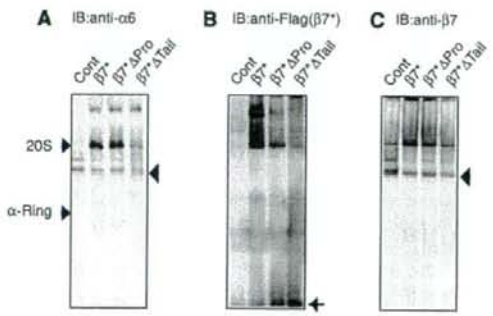

Figure 6 C-terminal tail of β7 is essential for the incorporation of β7 and dimerization of half-mers. Stable cell lines expressing the indicated mutant β7-subunits were treated with siRNA targeting endogenous β7. Cell extracts were resolved by native PAGE, followed by immunoblot analysis using the indicated antibodies. The free form of β7*Δtail is depicted by an arrow (**B**). The 'half-mer' assembly intermediates are depicted by arrowheads (**A, C**).

prerequisite for proteasome maturation in mammals, similar to the results in yeast. On the other hand, cells expressing β2*Δpro, β5*Δpro, β2*Δtail, and β7*Δtail were non-viable in the absence of their endogenous counterparts (data not shown), suggesting the indispensable roles of these propeptides and C-terminal tails in proteasome biogenesis in mammals.

Both the propeptide and C-terminal tail of β2 are required for incorporation of β3

To clarify the role of the propeptide and C-terminal tail of β2, extracts resolved by native PAGE were probed with several antibodies (Figure 4). β2*Δpro- and β2*Δtail-expressing cells showed accumulation of intermediates that included α6 and β2, indicating that β2 propeptide and β2 tail are not required for the incorporation of β2 itself (Figure 4A and B). However, these intermediates did not contain β3 (Figure 4C), suggesting that the assembly pathway is arrested before β3 incorporation and that both β2 propeptide and β2 tail are required for the incorporation of β3. PAC3 was also found in the intermediates in β2*Δpro cells and the faster migrating intermediates in β2*Δtail cells (indicated by an arrowhead), consistent with lack of β3 (Figure 4D). However, the slower migrating intermediates in β2*Δtail cells (indicated by the bar) did not include PAC3 (Figure 4D). These species did not contain any β-subunits other than β2Δtail (Supplementary Figure S6), precluding the possibility that loss of β2 tail and PAC3 causes disordered incorporation of β-subunits. Rather, it is likely that they represent either aggregation of intermediates or association of other molecules, which would be prevented in the presence of β2 tail or PAC3.

β5 propeptide is required for incorporation of β6 but not hUmp1-dependent proteasome maturation

Next, we examined the role of β5 propeptide. As expected from its lethality, β5*Δpro-expressing cells could not produce mature 20S proteasomes but showed accumulation of an intermediate that included α6 and β5, indicating that β5 propeptide is not essential for the incorporation of β5 itself (Figure 5A–C). This intermediate did not contain the next subunit β6 (Figure 5D) and represented the same size as the intermediate observed in β6-knockdown cells (Figure 5A and B), suggesting that β5 propeptide is required for the incorporation of β6 in mammalian cells.

In yeast, deletion of β5 propeptide, which is fatal, was rescued by concomitant loss of Ump1, suggesting the role of β5 propeptide in Ump1-dependent maturation of the yeast proteasome (Ramos *et al*, 1998). In the next series of experiment, siRNAs for both hUmp1 and β5 were transfected into β5*Δpro-expressing mammalian cells. Unlike the observation in yeast, however, simultaneous loss of β5 propeptide and hUmp1 was still lethal in mammalian cells, with the accumulation of an intermediate closely resembling to that observed in hUmp1 single-knockdown cells that did not contain β5* (Figure 5E and F). Although these results do not exclude the checkpoint function of hUmp1 as proposed in yeast Ump1 (Li *et al*, 2007), they confirm the important role of hUmp1 in the integrity of early assembly intermediates, which is a function independent of β5 propeptide.

Importance of C-terminal tail of β7 for stable incorporation of β7

β7*Δpro-expressing cells grew normal, incorporated β7*, and produced 20S proteasomes similar to wild-type β7*-expressing cells (Figure 6A–C). However, deletion of the C-terminal tail could not rescue loss of endogenous β7, and the cells could hardly produce 20S proteasomes (Figure 6A–C). In these cells, β7*Δtail failed to be incorporated in the assembly intermediates, presumably half-mers (Li *et al*, 2007), as suggested by the similar size as those in β7-knockdown cells and by the presence of β6 (Figure 6A and C, arrowheads) and accumulation of β7*Δtail as a free subunit (Figure 6B, arrow). These observations indicate that the C-terminal tail, which directly associates with the trans-β-ring, is essential for its stable incorporation into proteasomes and supports the model where β7 incorporation is tightly coupled with dimerization of half-mers, thus forming 20S proteasomes, as proposed in previous reports in yeast (Li *et al*, 2007; Marques *et al*, 2007).

Discussion

In the present study, we investigated in detail the assembly pathway of mammalian 20S proteasome and found a strictly ordered β-subunit incorporation, which was supported by propeptides of certain β-subunits. Starting from recruitment of β2 and hUmp1 on the α-ring, the adjacent β-subunit within the same β-ring, except β1, appears to assemble one after another, β7 being the last subunit whose incorporation is tightly coupled with dimerization of half-mers (see the model illustrated in Figure 7). This view is also supported by the observation that the size of the assembly intermediate in each knockdown cells increased as the maturation process proceeded (Figure 1A). The order of the β-subunit recruitment clarified in this study is entirely consistent with previous findings where β-subunits were separated into two categories; β2, β3, and β4 as 'early' subunits and others as 'late' subunits (Heinemeyer *et al*, 2004). In both yeast and mammals, the 13S complex containing β2, β3, β4, and (h)Ump1 was observed as a distinct assembly intermediate, suggesting that the following step, that is, incorporation of β5, is one of the rate-limiting steps in proteasome biogenesis. This may account for the intriguing observation that sole overexpression of β5 in mammalian cells increased the amount of assembled proteasomes (Chondrogianni *et al*, 2005). Although our data imply a stepwise addition of β-subunits on the α-ring, we cannot preclude the possibility that some β-subunits are incorporated as a group, for example as a β2–β3–β4–hUmp1 complex, under normal conditions as we observed intermediate species that can be seen only when a certain β-subunit is depleted.

β1 appears to be the last but one incorporated during proteasome assembly, which is a prerequisite for β7 incorporation. However, β1 can also be incorporated earlier than β4, β5, and β6 in the absence of these subunits, whereas the other subunits are assembled in a manner strictly dependent on the preceding incorporation of the neighbouring subunit. Although such β1-containing intermediates might be artefacts under non-physiological situations, this recalls the early assembly intermediate observed during immunoproteasome biogenesis, which contains β1i, β2i, β3, and β4 (Nandi *et al*, 1997). β1i is incorporated into the precursor earlier than β1,

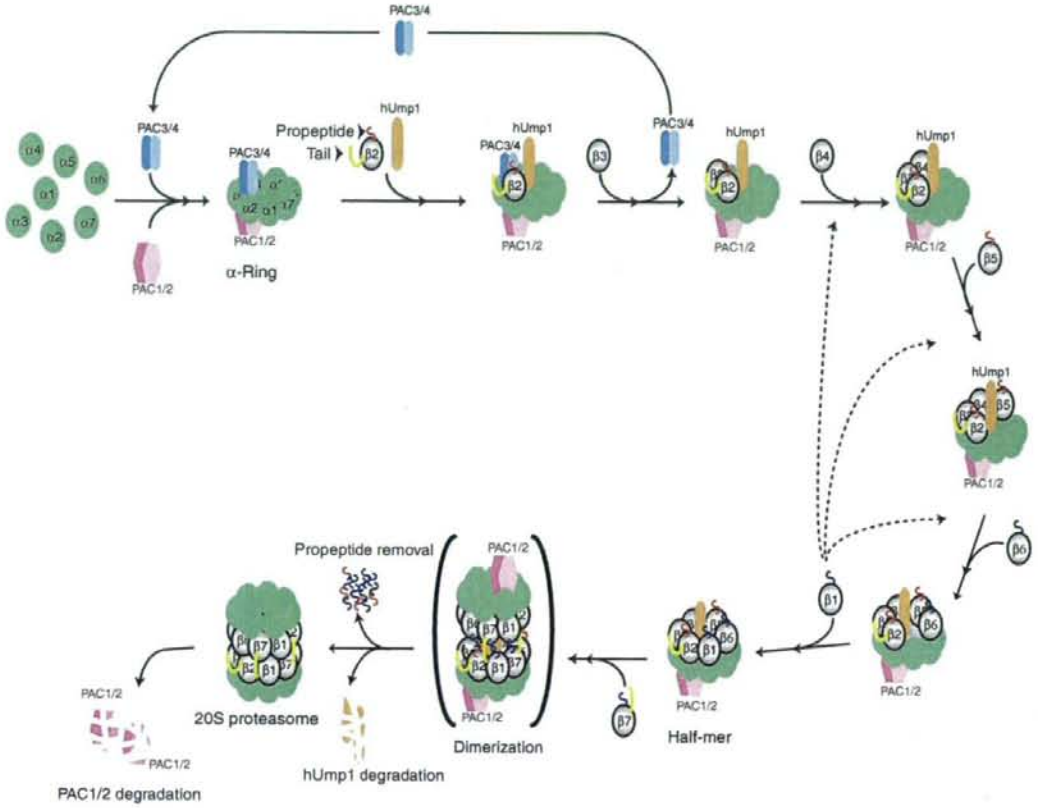

Figure 7 A model for β-ring formation in mammalian 20S proteasome assembly. The roles of PAC1–PAC2 and PAC3 in the formation of α-rings were described previously (Hirano *et al*, 2005, 2006). PAC4 was recently identified as a heterodimeric partner of PAC3 (Le Tallec *et al*, 2007). Sequential incorporation of β-subunits starts from the association of β2 and hUmp1 on the α-ring. hUmp1 is required for the association of β2 in the early assembly intermediates. PAC3–PAC4, whose release is coupled with association of β3, holds the structural integrity of the intermediates until β3 is incorporated on the α-ring. Subsequent orderly incorporation of other β-subunits is also assisted by intramolecular chaperones such as the propeptides of β2 and β5 and the C-terminal tail of β2. Although β1 can be incorporated at various steps (dotted lines), such incorporation most likely follows that of β6. Dimerization of half-mers is assisted by the C-terminal tail of β7. This is followed by removal of β-subunit propeptides (β1, β2, β5, β6, and β7) and hUmp1 degradation. Essential propeptides, non-essential propeptides, and essential C-terminal tails of β-subunits for mammalian 20S proteasome biogenesis are depicted in red, blue, and yellow, respectively. See text for more details.

which has an important function in the immunoproteasome assembly (Griffin *et al*, 1998).

In the present study, we identified several new roles for the propeptides and the C-terminal tails of mammalian β-subunits that have not been appreciated in those of yeast β-subunits. The propeptide of yeast β2 is dispensable for efficient proteasome biogenesis (Arendt and Hochstrasser, 1999), but that of mammalian β2 contributes to the recruitment of its neighbouring subunit β3 (Figure 4). The propeptide of yeast β5 is reported to be required for its own incorporation (Chen and Hochstrasser, 1996), whereas that of mammalian β5 was not; instead, its loss caused failure of β6 recruitment (Figure 5). The role of the C-terminal tail of mammalian β7 appears to be quite similar to that of yeast β7, but it proved to be an essential component in proteasome biogenesis, unlike yeast β7 (Figure 6).

Our study also clarified the sequences leading to hUmp1 incorporation and release of PAC3 from proteasome precursors. Incorporation of hUmp1 was as early as that of β2, the first β-subunit assembled on the α-ring. In the early assembly intermediates, hUmp1 unexpectedly had an important function in the association of β2 with the precursor proteasomes and proved to be a prerequisite for the assembly of β-subunits on the α-ring (Figures 3 and 7). This function is not appreciated for yeast Ump1, which regulates dimerization of half-proteasomes and maturation of 20S proteasomes, presumably by acting as a checkpoint protein (Ramos *et al*, 1998; Li *et al*, 2007). As the phenotype of loss of hUmp1 emerged at a stage upstream of the dimerization, we are uncertain whether hUmp1 in mammalian cells also has a function similar to that in yeast.

In a previous study, we showed that PAC3 was scarcely included in the complex purified by a tag attached to hUmp1 (Hirano *et al*, 2006). In the present study, we clarified that PAC3 release was coupled with association of β3 with the assembly intermediate. This observation is consistent with

the recent study showing that Dmp1–Dmp2, yeast orthologue of PAC3–PAC4, was copurified with β2, but not with other β-subunits (Yashiroda *et al*, 2008). Therefore, a complex containing both hUmp1 and PAC3, together with β2, is assumed to be present during the maturation pathway, and such a complex was indeed observed in β3-knockdown cells (Figure 1). As PAC3 is known to bind directly to β3 *in vitro* (Hirano *et al*, 2006), it may be argued that PAC3 facilitates the incorporation of β3, which might induce a conformational alteration of the assembly intermediate to release PAC3. Because PAC3 is also required for efficient α-ring formation (Hirano *et al*, 2006), we could not detect accumulation of an intermediate before the incorporation of β3 in PAC3-knockdown cells, such as a complex comprising α-ring and β2, which would be expected to occur on the assumption that PAC3 is required for β3 incorporation (Supplementary Figure S7). Although biochemical data both in yeast and mammals indicated that PAC3 is replaced when β3 enter, a model generated by superimposing Dmp1–Dmp2–α5 complex on the yeast 20S proteasome suggested steric hindrance of β4-subunit to Dmp1 (Yashiroda *et al*, 2008). The precise reason for this discrepancy is not clear at present. This may be simply because the model, which was based on the structure of Dmp1–Dmp2 determined in the absence of α-ring, does not represent bona fide structure of assembly intermediates. Further studies should be required for understanding the role of PAC3 in β-subunit incorporation.

Recently, the proteasome-specific inhibitor bortezomib was used clinically in refractory multiple myeloma, and a clinical trial of this agent in other malignant neoplasms is currently underway (Adams, 2004). Accordingly, the proteasome is now recognized as a potent target for cancer therapy (Adams, 2004). Assuming that inhibition of proteasome biogenesis is also beneficial in cancer therapy, it is important to understand the detailed mechanism of mammalian proteasome biogenesis. Our results could provide the foundation for the design and development of novel anticancer drugs that target proteasome biogenesis.

Materials and methods

DNA constructs

The cDNAs encoding β-subunits and those derivatives were cloned into pIRESpuro3 (Clontech) in frame with a C-terminal Flag tag. To make constructs for β-subunits resistant to siRNAs, synonymous mutagenesis in RNAi targeting sequences was performed using the QuikChange site-directed mutagenesis kit (Stratagene). Plasmids encoding β1*Δpro, β2*Δpro, β5*Δpro, β6*Δpro, and β7*Δpro were constructed by fusing human ubiquitin cDNA to the 5′ end of the cDNAs encoding mature forms of the corresponding subunits. In β2*Δtail and β7*Δtail, sequences encoding amino acids 244–277 and 248–264 were deleted, respectively. PCR was performed using Phusion DNA polymerase (Finnzymes), and all constructs were confirmed by sequencing.

Cell culture

HEK293T cell lines were cultured in Dulbecco's modified Eagle's medium (Sigma), supplemented with 10% fetal calf serum, 100 IU/ml penicillin G, 100 μg/ml streptomycin sulphate (all from Invitrogen). Stable transfection of HEK293T cells was performed using Fugene 6 (Roche), and the cells were selected with 5 μg/ml of puromycin (Sigma).

Protein extracts, immunological analysis, and antibodies

Cells were lysed in an ice-cold lysis buffer (50 mM Tris–HCl (pH 7.5), 0.5% (v/v) NP-40, 1 mM dithiothreitol, 2 mM ATP, and 5 mM $MgCl_2$) and the extracts were clarified by centrifugation at 20 000 *g* for 15 min at 4°C. The supernatants were subjected to glycerol gradient analysis or native PAGE. Glycerol gradient analysis and assay of proteasome activity were described previously (Murata *et al*, 2001; Hirano *et al*, 2006). *In vitro* binding assay was described previously (Hirano *et al*, 2006). SDS–PAGE (12% Bis-Tris gel (Invitrogen)) and native PAGE (7% Tris–acetate gel (Invitrogen)) were performed according to the instructions provided by the manufacturer. The separated proteins were transferred onto polyvinylidene difluoride membrane and reacted with the indicated antibody. Anti-PAC1, PAC2, PAC3, hUmp1, β4 (55F8), β5 (P93250), β6 (P93199), and PA28α polyclonal antibodies were described previously (Tanahashi *et al*, 2000; Hirano *et al*, 2006). Antibodies against proteasome α6 (MCP20), β1 (MCP421), β2 (MCP168), β3 (MCP102), β7 (MCP205), and PA200 were purchased from BioMol. Anti-Hsp90α and anti-Hsc70 were obtained from MBL. Anti-FLAG M2 antibody was from Sigma.

RNA interference

The siRNAs targeting human β-subunits and hUmp1 (Supplementary Table S1) were transfected into HEK293T cells using Lipofectamine RNAi MAX (Invitrogen) at a final concentration of 50 nM in six-well dishes twice at a 12-h interval. The cells were analysed 24 h after the second transfection.

Supplementary information

Supplementary data are available at *The EMBO Journal* Online (http://www.embojournal.org).

Acknowledgements

This study was supported by grants to SM and KT from the Ministry of Education, Science and Culture of Japan (MEXT), Target Protein Project of MEXT (to KT and KK), and the Takeda Science Foundation (KT).

References

Adams J (2004) The proteasome: a suitable antineoplastic target. *Nat Rev Cancer* **4:** 349–360

Arendt CS, Hochstrasser M (1999) Eukaryotic 20S proteasome catalytic subunit propeptides prevent active site inactivation by N-terminal acetylation and promote particle assembly. *EMBO J* **18:** 3575–3585

Baumeister W, Walz J, Zuhl F, Seemuller E (1998) The proteasome: paradigm of a self-compartmentalizing protease. *Cell* **92:** 367–380

Chen P, Hochstrasser M (1996) Autocatalytic subunit processing couples active site formation in the 20S proteasome to completion of assembly. *Cell* **86:** 961–972

Chondrogianni N, Tzavelas C, Pemberton AJ, Nezis IP, Rivett AJ, Gonos ES (2005) Overexpression of proteasome beta5 assembled subunit increases the amount of proteasome and confers ameliorated response to oxidative stress and higher survival rates. *J Biol Chem* **280:** 11840–11850

Coux O, Tanaka K, Goldberg AL (1996) Structure and functions of the 20S and 26S proteasomes. *Annu Rev Biochem* **65:** 801–847

Fehlker M, Wendler P, Lehmann A, Enenkel C (2003) Blm3 is part of nascent proteasomes and is involved in a late stage of nuclear proteasome assembly. *EMBO Rep* **4:** 959–963

Frentzel S, Pesold-Hurt B, Seelig A, Kloetzel PM (1994) 20S proteasomes are assembled via distinct precursor complexes. Processing of LMP2 and LMP7 proproteins takes place in 13–16S preproteasome complexes. *J Mol Biol* **236:** 975–981

Glickman MH, Ciechanover A (2002) The ubiquitin-proteasome proteolytic pathway: destruction for the sake of construction. *Physiol Rev* **82:** 373–428

Griffin TA, Nandi D, Cruz M, Fehling HJ, Kaer LV, Monaco JJ, Colbert RA (1998) Immunoproteasome assembly: cooperative incorporation of interferon gamma (IFN-gamma)-inducible subunits. *J Exp Med* **187:** 97–104

Groll M, Ditzel L, Lowe J, Stock D, Bochtler M, Bartunik HD, Huber R (1997) Structure of 20S proteasome from yeast at 2.4 Å resolution. *Nature* **386:** 463–471

Heinemeyer W, Ramos PC, Dohmen RJ (2004) The ultimate nanoscale mincer: assembly, structure and active sites of the 20S proteasome core. *Cell Mol Life Sci* **61:** 1562–1578

Hirano Y, Hayashi H, Iemura S, Hendil KB, Niwa S, Kishimoto T, Kasahara M, Natsume T, Tanaka K, Murata S (2006) Cooperation of multiple chaperones required for the assembly of mammalian 20S proteasomes. *Mol Cell* **24:** 977–984

Hirano Y, Hendil KB, Yashiroda H, Iemura S, Nagane R, Hioki Y, Natsume T, Tanaka K, Murata S (2005) A heterodimeric complex that promotes the assembly of mammalian 20S proteasomes. *Nature* **437:** 1381–1385

Imai J, Maruya M, Yashiroda H, Yahara I, Tanaka K (2003) The molecular chaperone Hsp90 plays a role in the assembly and maintenance of the 26S proteasome. *EMBO J* **22:** 3557–3567

Jager S, Groll M, Huber R, Wolf DH, Heinemeyer W (1999) Proteasome beta-type subunits: unequal roles of propeptides in core particle maturation and a hierarchy of active site function. *J Mol Biol* **291:** 997–1013

Kusmierczyk AR, Kunjappu MJ, Funakoshi M, Hochstrasser M (2008) A multimeric assembly factor controls the formation of alternative 20S proteasomes. *Nat Struct Mol Biol* **15:** 237–244

Le Tallec B, Barrault MB, Courbeyrette R, Guerois R, Marsolier-Kergoat MC, Peyroche A (2007) 20S proteasome assembly is orchestrated by two distinct pairs of chaperones in yeast and in mammals. *Mol Cell* **27:** 660–674

Li X, Kusmierczyk AR, Wong P, Emili A, Hochstrasser M (2007) Beta-subunit appendages promote 20S proteasome assembly by overcoming an Ump1-dependent checkpoint. *EMBO J* **26:** 2339–2349

Marques AJ, Glanemann C, Ramos PC, Dohmen RJ (2007) The C-terminal extension of the beta 7 subunit and activator complexes stabilize nascent 20s proteasomes and promote their maturation. *J Biol Chem* **282:** 34869–34876

Murata S (2006) Multiple chaperone-assisted formation of mammalian 20S proteasomes. *IUBMB Life* **58:** 344–348

Murata S, Sasaki K, Kishimoto T, Niwa S, Hayashi H, Takahama Y, Tanaka K (2007) Regulation of CD8+ T cell development by thymus-specific proteasomes. *Science* **316:** 1349–1353

Murata S, Udono H, Tanahashi N, Hamada N, Watanabe K, Adachi K, Yamano T, Yui K, Kobayashi N, Kasahara M, Tanaka K, Chiba T (2001) Immunoproteasome assembly and antigen presentation in mice lacking both PA28alpha and PA28beta. *EMBO J* **20:** 5898–5907

Nandi D, Woodward E, Ginsburg DB, Monaco JJ (1997) Intermediates in the formation of mouse 20S proteasomes: implications for the assembly of precursor beta subunits. *EMBO J* **16:** 5363–5375

Preckel T, Fung-Leung WP, Cai Z, Vitiello A, Salter-Cid L, Winqvist O, Wolfe TG, Von Herrath M, Angulo A, Ghazal P, Lee JD, Fourie AM, Wu Y, Pang J, Ngo K, Peterson PA, Fruh K, Yang Y (1999) Impaired immunoproteasome assembly and immune responses in PA28−/− mice. *Science* **286:** 2162–2165

Ramos PC, Hockendorff J, Johnson ES, Varshavsky A, Dohmen RJ (1998) Ump1p is required for proper maturation of the 20S proteasome and becomes its substrate upon completion of the assembly. *Cell* **92:** 489–499

Ramos PC, Marques AJ, London MK, Dohmen RJ (2004) Role of C-terminal extensions of subunits beta2 and beta7 in assembly and activity of eukaryotic proteasomes. *J Biol Chem* **279:** 14323–14330

Schmidtke G, Schmidt M, Kloetzel PM (1997) Maturation of mammalian 20S proteasome: purification and characterization of 13S and 16S proteasome precursor complexes. *J Mol Biol* **268:** 95–106

Tanahashi N, Murakami Y, Minami Y, Shimbara N, Hendil KB, Tanaka K (2000) Hybrid proteasomes. Induction by interferon-gamma and contribution to ATP-dependent proteolysis. *J Biol Chem* **275:** 14336–14345

Tanaka K, Kasahara M (1998) The MHC class I ligand-generating system: roles of immunoproteasomes and the interferon-gamma-inducible proteasome activator PA28. *Immunol Rev* **163:** 161–176

Unno M, Mizushima T, Morimoto Y, Tomisugi Y, Tanaka K, Yasuoka N, Tsukihara T (2002) The structure of the mammalian 20S proteasome at 2.75 Å resolution. *Structure (Camb)* **10:** 609–618

Witt E, Zantopf D, Schmidt M, Kraft R, Kloetzel PM, Kruger E (2000) Characterisation of the newly identified human Ump1 homologue POMP and analysis of LMP7(beta 5i) incorporation into 20S proteasomes. *J Mol Biol* **301:** 1–9

Yashiroda H, Mizushima T, Okamoto K, Kameyama T, Hayashi H, Kishimoto T, Niwa S, Kasahara M, Kurimoto E, Sakata E, Takagi K, Suzuki A, Hirano Y, Murata S, Kato K, Yamane T, Tanaka K (2008) Crystal structure of a chaperone complex that contributes to the assembly of yeast 20S proteasomes. *Nat Struct Mol Biol* **15:** 228–236